CHAPTER 4

Changes to the Hydrological Connectivity and Their Effects on the Hydrology of a Wetland

4.1 Introduction

Hydrological connectivity can be described as the water-mediated transfer of matter, energy and/or organisms within or between elements of the hydrological cycle (Pringle 2003). Such a general description allows for a four-dimensional conceptualisation of the connectivity of lotic ecosystems that includes three spatial dimensions (lateral, longitudinal and vertical) plus a temporal dimension (Ward 1989).

Longitudinal and lateral hydrological connectivity are factors influencing interactions between adjacent aqueous bodies because they determine the magnitude and frequency of the changes that occur in the abiotic and biotic ecosystems of both bodies. This has been shown to apply to river-floodplain ecosystems in Austria (Heiler et al. 1995; Tockner et al. 1999), Australia (Marshall et al. 2006; Thoms 2003), and the United States (Freeman et al. 2006). It also applies for interactions between coastal wetlands and their estuaries in the United States (Cahoon 1994; Chambers et al. 1999), Australia (Johnson et al. 2004; Leigh & Sheldon 2008), and coral reefs and their surrounding systems in the Caribbean (Mumby & Harborne 1999) and Australia (Leis 2002). An estuarine ecosystem is dominated by a regular periodic tidal cycle that exceeds the effects of the vertical movements of evaporation, transpiration and groundwater absorption. Although rainfall is also a vertical movement, its main influence in an estuary is the horizontal runoff from the catchment areas; hence, this chapter focuses on the longitudinal dimension of hydrological connectivity.

Despite the importance of hydrological connectivity, anthropogenic structures have had a significant effect on this process worldwide. Globally, one-half of all the accessible freshwater runoff from rivers has been appropriated by humans (Postel et al. 1996) and 98% of all US streams have had their hydrological connectivity

compromised by anthropologenic structures (Benke 1990). In Australia, 446 large dams, 10,000 weirs and countless irrigation structures have fragmented floodplain-river ecosystems (Kingsford 2000). In NSW, 1035 floodgates influence the hydrology of coastal wetlands, and the Macleay River, the focus of this study, has 352 floodgates and 34 km of levee banks controlling all the estuarine streams (Webb et al. 1999).

The consequences of these modifications to hydrological connectivity are described in Chapter 2.

Globally, there is increasing interest in the restoration of coastal wetlands by tidal re-inundation (Turner & Lewis 1996; Zedler 2000). The benefits of this process, such as the repopulation by the original estuarine flora and fauna species and the buffering effects of saline water on acid sulfate soils, are now well established (Glamore & Indraratna; Zedler 2001). One of the negative consequences of this technique is the intrusion of the saline water onto agricultural land, but techniques to overcome this difficulty are continually being developed (Boumans et al. 2002; Glamore & Indraratna 2004; Greenwood & McFarlane 2006; Haines 2013; Howe et al. 2009; Montalto 2005; Nelson 2006; Portney & Giblin 1997; Williams & Watford 1997; Zedler 2000).

This study focuses on the changes to the Yarrahapinni Wetland ecosystem that occurred as a result of an incremental restoration of tidal hydrological connectivity. The significant features affecting the wetland's hydrology are:

1. the enclosing levee bank and a floodgate structure that has been progressively opened to re-establish tidal hydrological connectivity,
2. partial fragmentation of the wetland by stands of *Phragmites australis* that are slowly deteriorating with the influx of saline water,
3. a region in the upper reaches that is totally disconnected by a reed bank from the rest of the wetland and acts as a freshwater dam.

A schematic representation of the hydrology of the wetland is shown in Figure 4.1. The green arrows represent magnitudes of the incoming tidal flow, which is progressively diminished by the floodgate structure and phragmites beds as it moves into the

wetland. The black arrows represent freshwater outflow, which is controlled by major rainfall events. This results in the wetland being in a constant cycle of flooding and recovery.

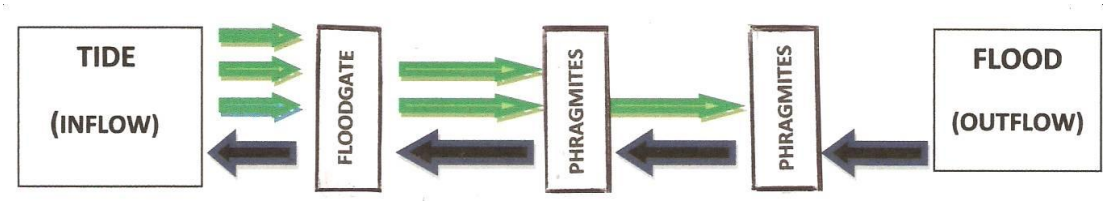

Figure 4.1: A schematic wetland hydrology model for the Yarrahapinni Wetland

The aim of this chapter is to quantify hydrological connectivity in relation to the tidal input and runoff output, and its effects on the chemical and physical hydrology of the Yarrahapinni Wetland.

To achieve this aim the following objectives are addressed:

1. Specify the percentages of the oceanic tidal range and tidal prism entering the Macleay River that are available for tidal restoration of the wetland.
2. Establish a mathematical relationship to quantify the tidal hydrological connectivity of the various floodgate opening configurations and their correlation with the wetland's hydrological properties.
3. Determine the role of the changing blockages of *Phragmites australis* on the hydrology and water quality of the wetland.
4. Quantify the relationship between rainfall in the catchment area of the wetland and the water level within the impounded freshwater area in the wetland's upper reaches.
5. Establish the correlations between water level in this freshwater section and the chemical hydrology of the remainder of the wetland.
6. Specify the quantitative nature of the salinity recovery of the wetland following flooding events.

7. Monitor the changes occurring in the acid sulfate soil areas within the wetland as a result of increasing hydrological connectivity and their effects on the chemical hydrology.

4.2 Study Area: History of Hydrological Connectivity Changes

The history of the hydrological connectivity of the Yarrahapinni Wetland can be summarised in five different stages (see Fig. 4.2 for study area location):

- Stage 0: pre-flood mitigation—the natural state,
- Stage 1: after-flood mitigation—1970 to December 2007,
- Stage 2: start of trial openings on 4 December 2007 to 5 February 2010,
- Stage 3: 5 February 2010 to 24 July 2011, (further gate opening).
- Stage 4: 24 July 2011 to the present, (last gate opening)

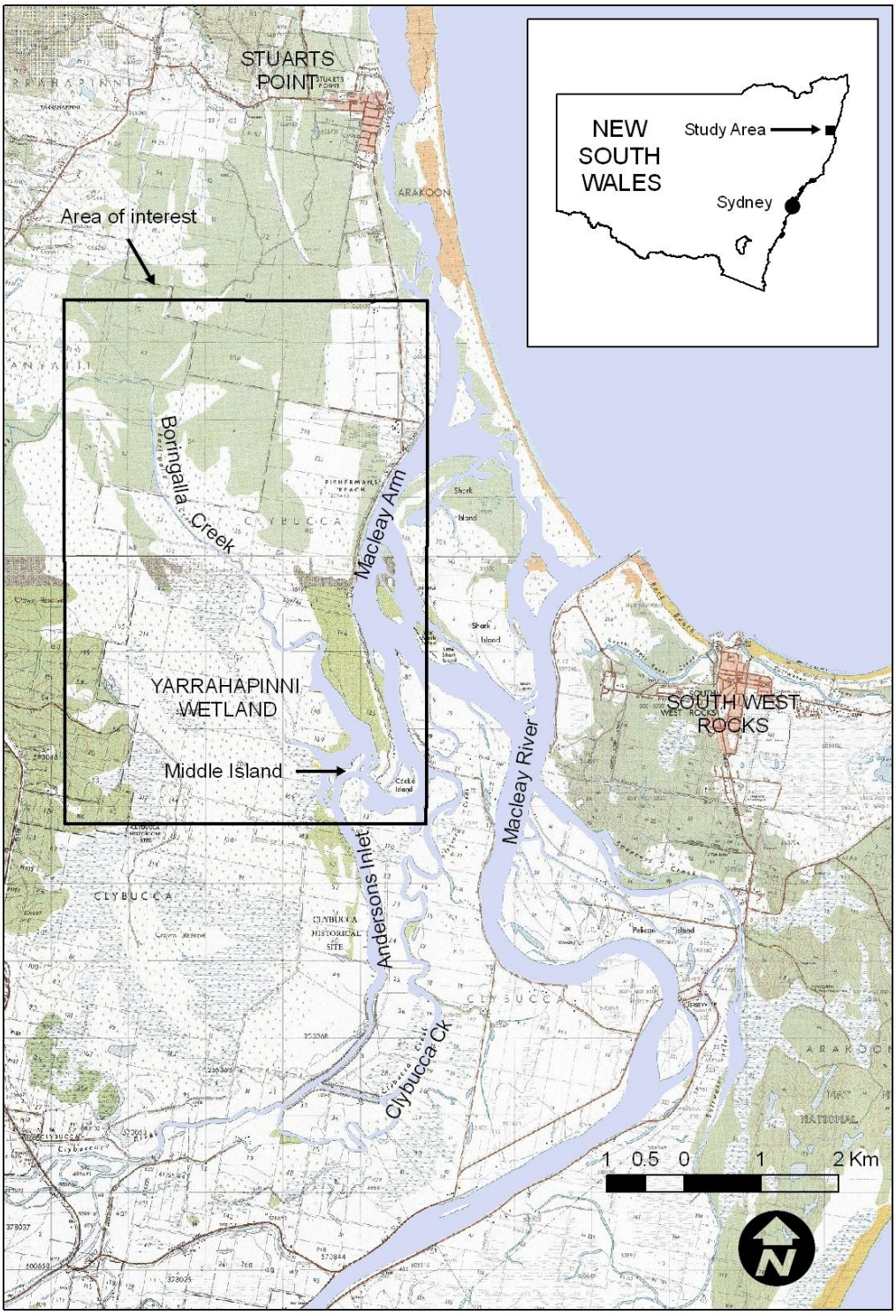

Figure 4.2: Study area site location (NPWS, 2012)

4.2.1 Stage 0: Pre-Flood Mitigation—The Natural State

Prior to the flood mitigation program, which commenced construction in 1970, the Yarrahapinni Wetland region was composed of a small mangrove creek (Middle Creek), a large mangrove creek (Borirgalla Creek) and a wide, open shallow area, with a sand substratum, known as the Broadwater (Fig. 4.3). The region was separated from Andersons Inlet by a row of mangrove islands and tidal inflow was achieved by flow through five shallow channels between the islands. The upper reaches of Borirgalla Creek above tidal influence consisted of a large freshwater wetland that merged with agricultural properties and varied considerably in extent between wet and dry periods.

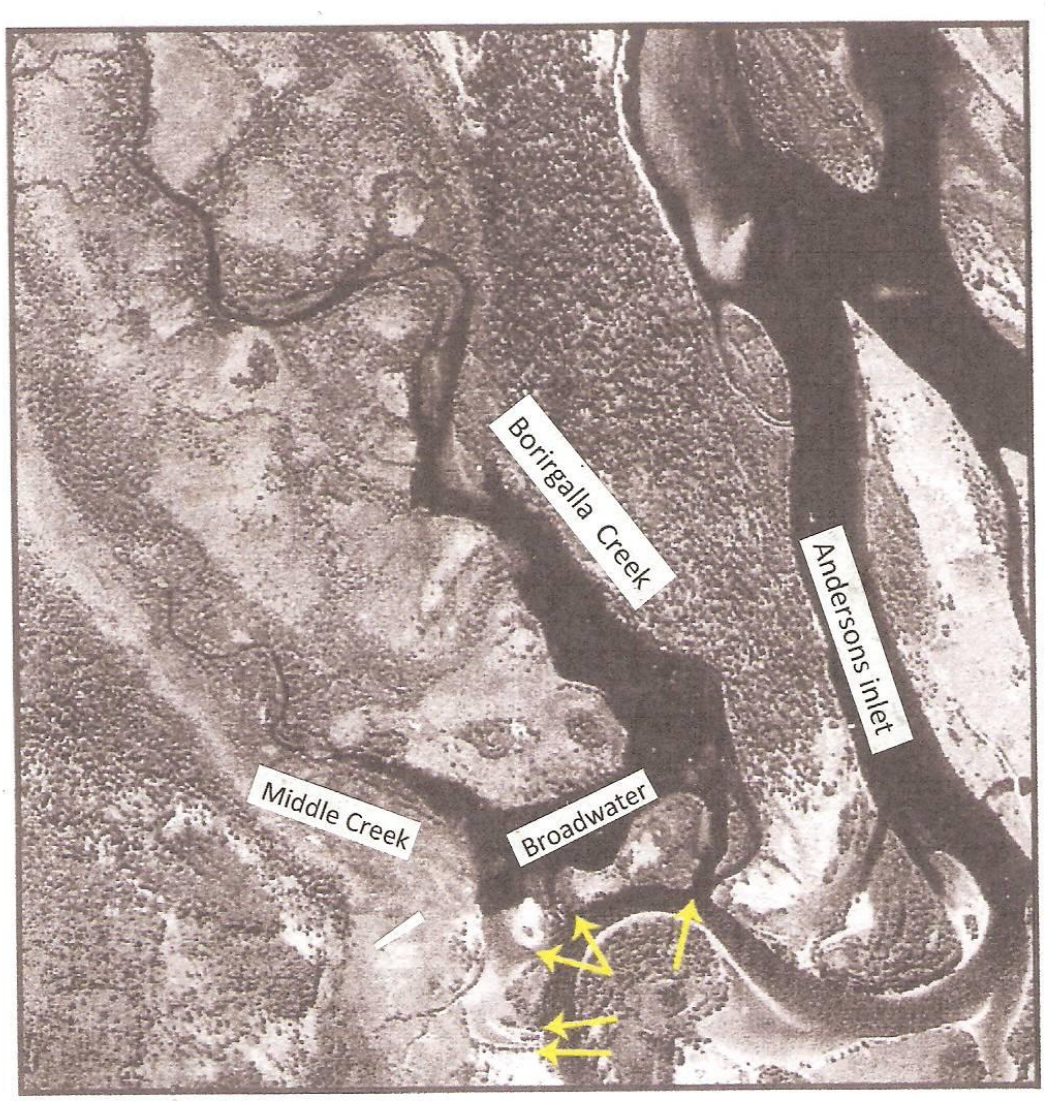

Source: NSW DECC

Figure 4.3: Aerial photograph of Yarrahapinni Wetland (1967) showing the area of interest highlighted in Figure 4.2

The five channels from Andersons Inlet are indicated with yellow arrows

4.2.2 Stage 1: After Flood Mitigation: 1970 to December 2007

The majority of the flood mitigation program structural alterations to the Yarrahapinni wetlands were performed during 1970 and 1971. The changes to the hydrological connectivity can be summarised into three major modifications:

1. A 900-m levee was constructed that joined the mangrove islands that closed the mouths of the five inlets shown in Stage 0, and excluded tidal exchange between the wetland and Andersons Inlet (Fig. 4.4).

Figure 4.4: Aerial photograph (1976) of the same region after flood mitigation work The white arrows indicate the position of the enclosing levy wall and the red arrows indicate the position of the auxiliary channel and floodgate structure.

2. A small added channel was constructed to accommodate a floodgate structure. This consisted of a 10-m long concrete culvert to which five steel, 2 x

2.7 m, top-hinged floodgates were added to allow outflow but stop tidal inflow (Fig. 4.5).

Figure 4.5: Inside view of the floodgate structure November 2007

3. Approximately 4 km of drainage channels through the upper section of the larger mangrove creek, Borirgalla Creek, and the lower regions of surrounding agricultural properties were constructed. The stated aim of these constructions was to increase the hydrological connectivity for runoff from rainfall and improve the drainage of agricultural land.

During the later part of Stage 1, a number of hydrological surveys were performed by the MHL, Sydney. These were:

1. MHL, 2001, DLWC Water Quality Monitoring at Yarrahapinni Wetland, MHL Report 986, Manly, NSW,
2. MHL, 2002, DLWC Water Quality Monitoring at Yarrahapinni Wetland, MHL Report 1151, Manly, NSW,
3. MHL, 2004, DIPNR Macleay River Estuary Tidal Data Collection April–May 2003, MHL Report 1250, MHL, NSW.

These reports contain data such as the variation of tidal heights and tidal flow rates for various positions in the Macleay River and its estuaries. When analysed, this provides valuable information about the Yarrahapinni Wetland and its external estuaries prior to the attempt at tidal re-inundation.

Two parameters that provide an indication of the water available externally to the floodgates and available for the tidal re-inundation are the tidal range and the tidal prism. A tidal prism refers to the total volume of water that flows past a given point within the estuary in a 24-hour period. The tidal pulse reaching the area of Andersons Inlet adjacent to the floodgates travels approximately 7 km from the ocean. There is an initial loss of tidal range at the shallow river entrance; it then passes through an approximately 130-m wide channel into the Macleay Arm—a shallow sill with a narrow navigation channel into Andersons Inlet and an extensive sill with no channel, downstream from the floodgates. Losses in volumes of tidal flow volume at these discontinuities can be shown from tidal prism results from this survey (Table 4.1).

Table 4.1: Tidal prisms at various stations within the Macleay River (MHL 2004)

POSITION	INFLOW TIDAL PRISMm^3 x 10^6	PERCENTAGE %
Inside Macleay River entrance	16.65	100
Macleay Arm	7.22	43
Clybucca Creek	2.31	14
Andersons Inlet	1.73	10

The positions for these results are shown in Figure 4.6.

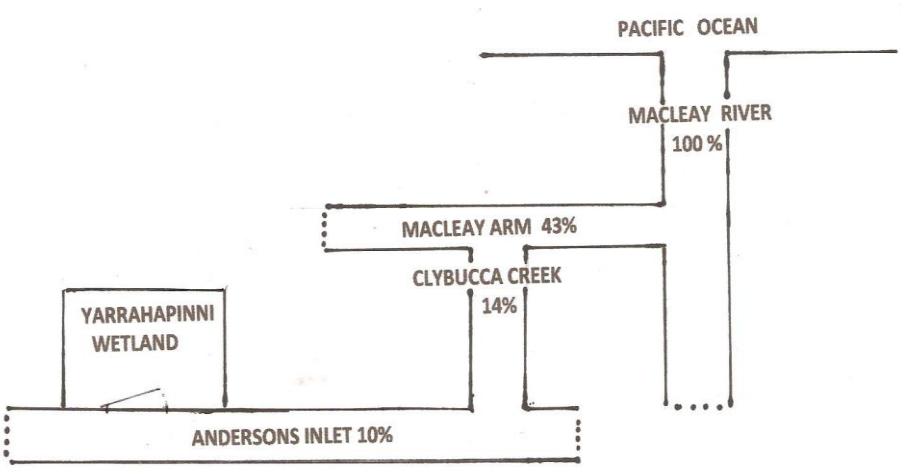

Figure 4.6: Schematic diagram of the connectivity of saline ocean water at the various positions in the Macleay River in terms of the tidal prisms

Tidal ranges from the same survey, at these locations, are shown in Figure 4.7.

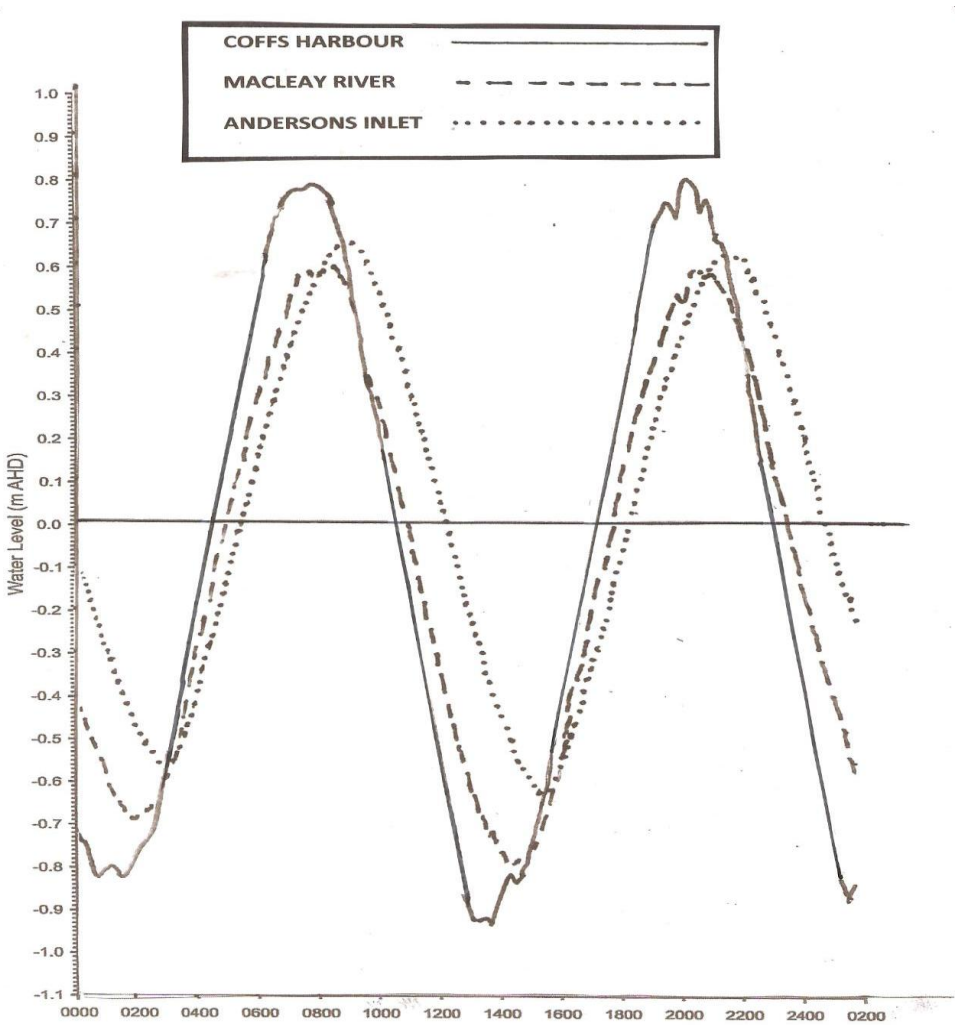

Eastern Standard Time 16 April 2003

Figure 4.7: Comparison of tidal ranges in the ocean, Macleay River and Andersons Inlet (MHL 2004)

These results are summarised in Table 4.2

Table 4.2: Comparisons of tidal ranges for the ocean, Macleay River, Macleay Arm and Andersons Inlet for 16 April 2003 (MHL2004)

POSITION	TIDAL RANGE m		COMPARISON WITH OCEAN %
	1st Tidal Cycle	2nd Tidal Cycle	
Ocean	1.62	1.75	100
Macleay River	1.30	1.41	80.3
Macleay Arm	1.22	1.24	73.0
Andersons Inlet	1.26	1.28	75.4

The results in Table 4.2 show that there is a 19.7% reduction in tidal range across the river mouth, a further 7.3% loss entering the Macleay Arm but a 2.4% rise to the Yarrahapinni floodgates, indicating a tidal amplification for Andersons Inlet. This survey by the MHL was performed for one day only and these results would vary considerably for other tidal cycles of different magnitude. The predicted tidal cycle ranges for 16 April 2003 were 1.52 m and 1.65 m, and both high tides were predicted to be 0.77 m above Australian Height Datum (AHD) (MHL 2002).

It is also possible to derive some information on the state of hydrological connectivity at the floodgates prior to the opening trials. Connectivity at the floodgates for Stage 1 should be 0 because all five floodgates had been shut for approximately 36 years, except for temporary openings for maintenance or as the result of vandalism. There has been some inflow from the overtopping of the levy by very high tides, leakage due to porosity in the levy walls and leakage in the gate seals. This inflow is mainly restricted to periods of very high tides.

The tides in eastern Australia vary in a 14-day cycle. Twice a lunar month (approximately 28 days), around the full moon and the new moon, the tides display a higher tidal range than normal (spring tides). Approximately seven days later than the spring tides, very small tidal ranges occur (neap tides).

The MHL installed data loggers to record water levels, pH and salinity at sites outside the floodgate structure and at Middle Island, inside the wetland, for the period 1996 to 1999 (MHL 2001). The data show an approximately 14-day tidal cycle within the wetland. For a few days during the high spring tides, the tidal difference on either side of the floodgates is sufficient to allow small rises in tidal height inside the wetland. Approximately seven days later, during the neap tides, the reverse process occurs and the tidal height within the wetland falls in very small steps for a few days. Figures 4.8 and 4.9 show comparisons of the sinusoidal tidal levels outside the floodgates with the water level within the wetland for two four-day periods during November 1996. These figures show the very small, stepped rise and fall of the tidal height within the wetland. The two periods are shown separately for the sake of clarity because the changes are so small.

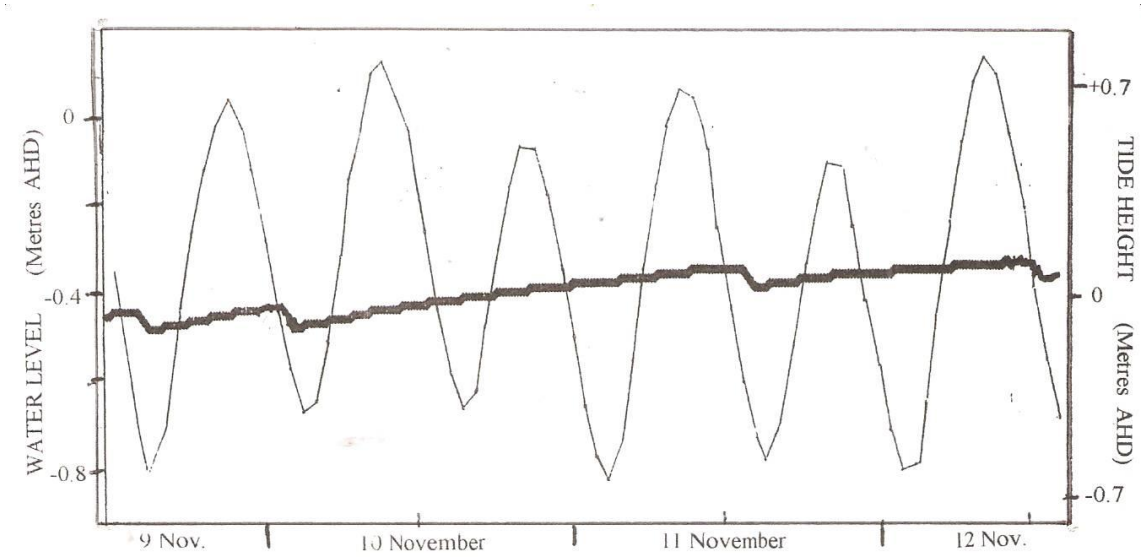

Figure 4.8: Comparison of the water level within the wetland with the tidal levels outside the floodgates for a period of rising water levels (MHL 2001)

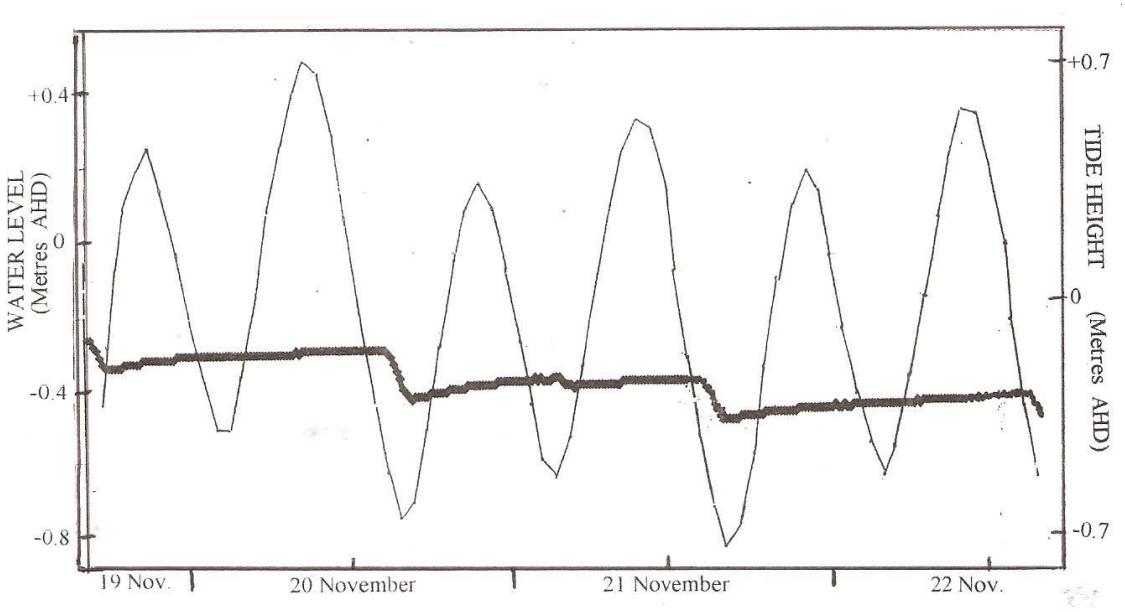

Figure 4.9: Comparison of the water level within the wetland with the tidal levels outside the floodgates for a period of falling water levels (MHL 2001)

Figure 4.10 shows the water levels for the period from 19 December 2004 to 1 January 2005 at the Middle Island data logger site M1. This period of data was chosen because it demonstrates one of the periods of maximum water level variations available in previous data.

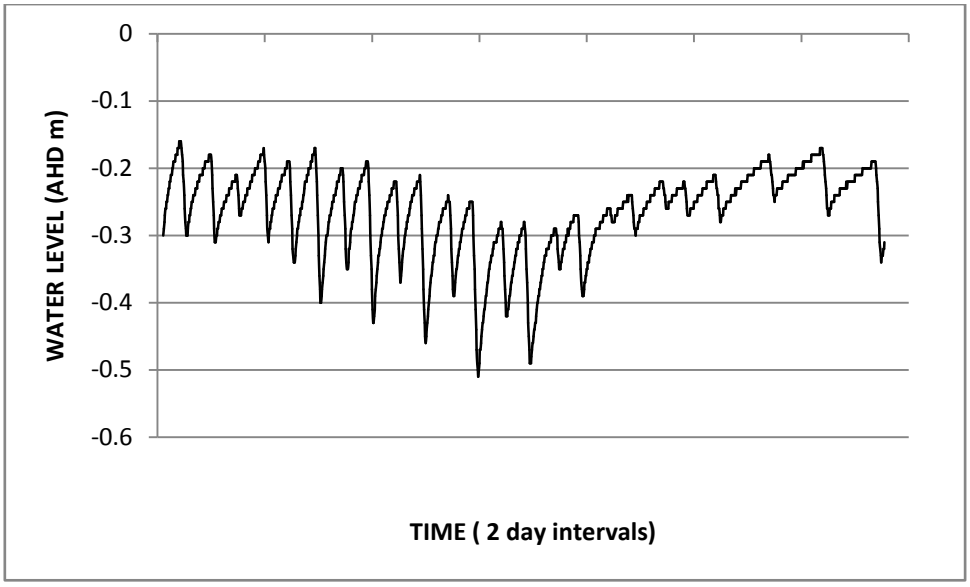

Figure 4.10: Water levels at Site M1 for a 14-day period commencing 19 December 2004 (MHL 2004)

4.2.3 Stage 2: Start of Trial Openings 4 December 2007 to 5 February 2010

The first of the incremental floodgate openings consisted of replacing the two eastern floodgates with self-regulating Armon floodgates. These consisted of each 2.0 x 2.7 m gate having a central 0.8 x 0.5 m opening that is fitted with a float-operated flap designed to close the opening when the incoming high tide reaches a predetermined level. The dimensions of each gate and their positioning are shown in Figure 4.11, and the self-opening mechanism is shown in Figure 4.12.

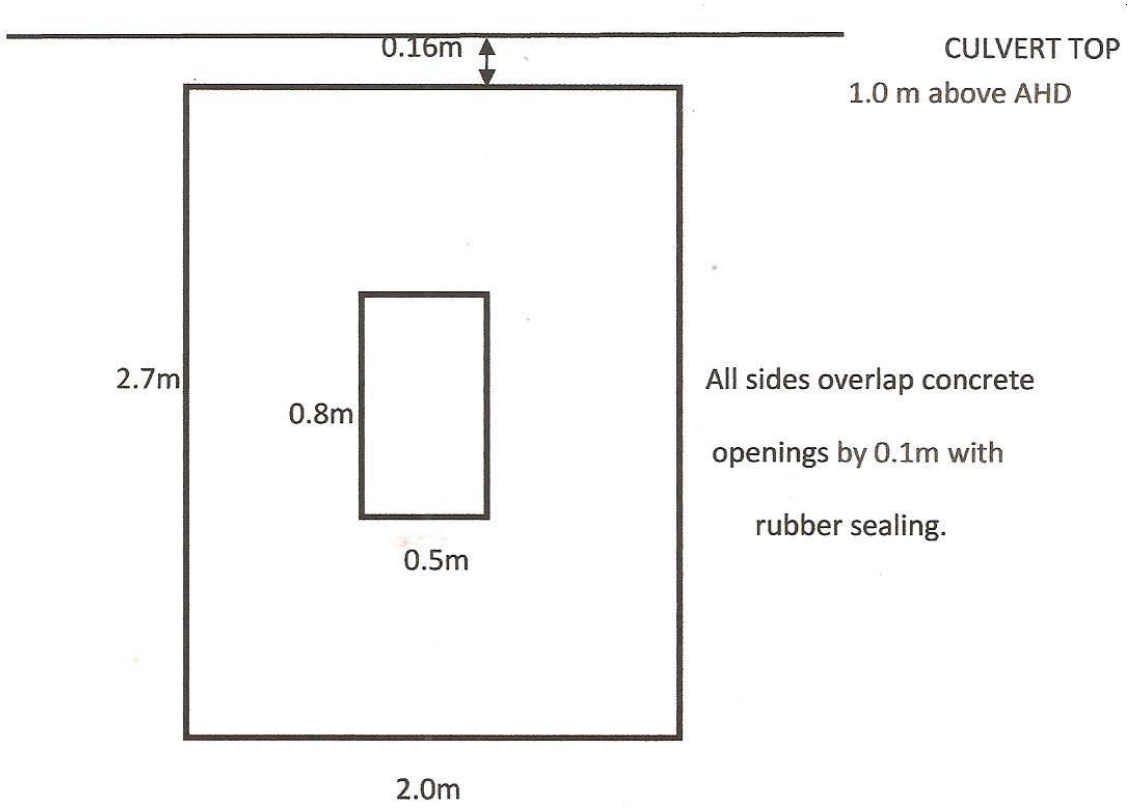

Figure 4.11: Dimensions and position of each gate and the smaller opening

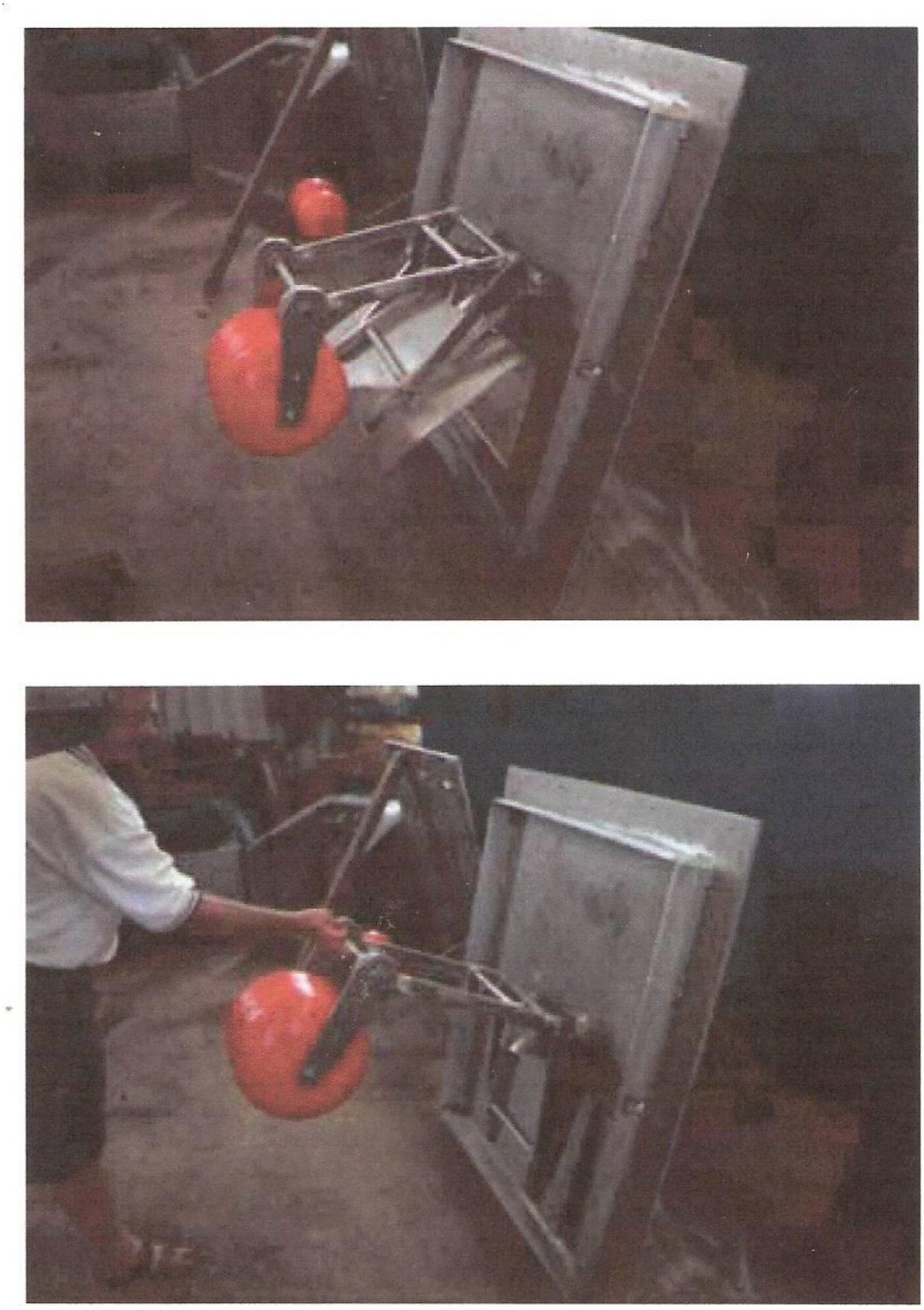

Figure 4.12: Float-operated floodgate manufactured by Armon Engineering, Kempsey, upper: gate position at low tide, lower: gate position at high tide (Kroon et al. 2004) (note: gates shown have opening at a lower level than those fitted)

The float mechanisms were subject to vandalism on a number of occasions and both float mechanisms had been completely removed by 1 July, leaving a 0.4 m^{-2} central opening in both gates.

4.2.4 Stage 3: 5 February 2010 to 24 July 2011

The culvert structure supporting the floodgates was fitted with a lifting frame on the outside that has cables attached enabling the floodgates to be individually raised. One of the gates with the small opening was raised on 5 February 2010, allowing full tidal flow through one of the five culvert openings.

4.2.5 Stage 4: 24July 2011 to the Present

On 24 July 2011, the gates again suffered vandalism by the attempted removal of two of the closed gates through removal of the supporting bolts. The two gates were then totally removed by controlling authorities (Fig. 4.13).

Figure 4.13: Status of floodgate openings for Stage 4

4.3 Data Analysis: Theoretical Context

Hydrological connectivity in a natural river system is often controlled by complex interactions of many variables and is difficult to quantify. These key variables can include the irregular nature and lengths of the natural restrictions to connectivity, varying stream depths, morphology and roughness, and variations in flow rates and quantities due to floods or droughts (Kadlec 1990; Reid et al. 2012; Wagenschein & Rode 2008; Ward & Stanford 1995).

Varying techniques have been used to relate hydrological connectivity to other factors that are easier to quantify in a particular situation. These include relating hydrological connectivity to a transect height related area rating (Westgate et al. 2012), using a measure of 23 landscape metrics to develop a connectivity scale of 0 to 1 (Van Nieuwenhuyse et al. 2011) and a computer model using overbank flooding height and time of overtopping to develop a scale for hydrological connectivity (Karim et al. 2012).

In the case of anthropogenic obstructions to hydrological connectivity such as dams, weirs and floodgates, most of these difficulties in quantification no longer apply. The longitudinal connectivity distance across such a structure is short, constant in cross-section and thus easy to measure, and very low in roughness classification.

The driving force for longitudinal hydrological connectivity through an opening in such a structure is the difference between the hydrostatic pressures on either side of its connectivity opening. Hydrostatic pressure is directly proportional to the depth of an incompressible fluid, such as water, so it is usually more convenient to refer to the height of the fluid or its 'hydraulic head' and use units of distance (Fig. 4.14).

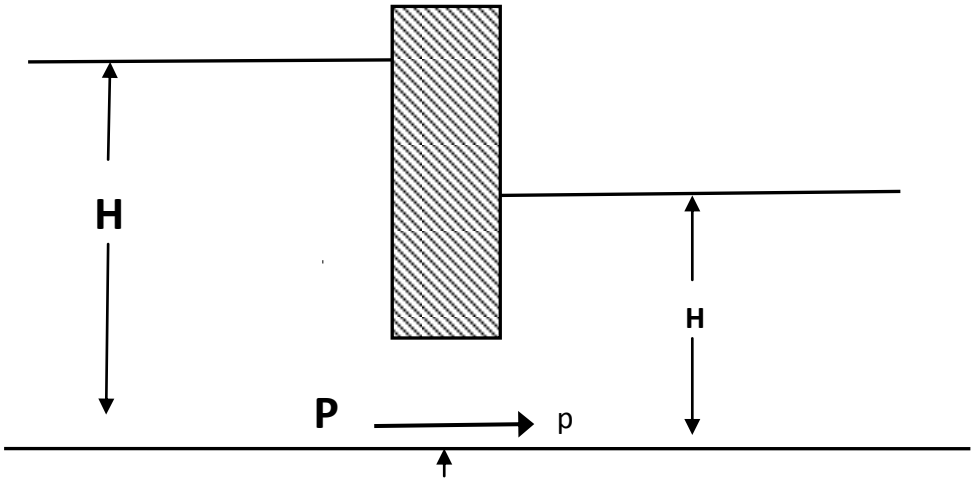

Figure 4.14: Schematic representation of hydrological connectivity through an anthropogenic obstruction

P = the upstream hydrostatic pressure, P = the downstream hydrostatic pressure, H = the upstream fluid 'Head' and H represents the downstream fluid 'Head'

In the case of an estuarine waterway that involves tidal flow, this simple model is complicated by the upstream body of water exhibiting high and low tides in anapproximately sinusoidal waveform. In coastal NSW, there are two high tides and two low tides a day, which follow an approximately 28-day cycle of varying magnitudes (MHL 2000–2013). It also is more complicated if the structure involved is a floodgate. These are usually on the upstream side of the culvert, and top hinged and free swinging so they only restrict incoming tides and are free to swing open from hydrostatic pressure differential during the outgoing tides (Middleton et al. 1985; Pollard & Hannan 1993; Pressey & Middleton 1982).

The changes to hydrological connectivity at the floodgates were quantified for the various stages by comparing the area of the gates opened with the opening available if all floodgates were removed, using the formula:

$$\% \text{ Hydrological Connectivity} = \frac{\text{Area of opening}}{\text{Area with all gates open}} \times 100$$

The area for a small 0.8 x 0.5 m opening is 0.4 m^2 and, for a full opening, the area is the dimensions of each opening in the concrete culvert: 2.4 x 1.8 m, or 4.32 m^2.

Results derived from this formula must only be taken as an indication because a more accurate formula would have to take into account the change of the opening at various tidal heights and the resulting differences between the hydraulic head on either side of the gates. The approximations of hydrological connectivity at the various stages are shown in Table 4.3.

Table 4.3: Approximate connectivity for the various opening configurations

	GATE NUMBER (from east)					Connectivity
	5	4	3	2	1	%
Stage 1	Shut	Shut	Shut	Shut	Shut	0
Stage 2	Shut	Shut	Shut	Small	Small	4
Stage 3	Shut	Shut	Open	Shut	Small	24
Stage 4	Open	Open	Shut	Open	Open	63

4.4 Data Sources and Methods

Hydrological data were collected from a variety of sources:

1. Hourly water level recordings within the wetland were obtained for the period from December 2007 to December 2012 utilising 18 Odyssey Capacitance Water Level Probe data loggers. Not all of these were used simultaneously; numerous replacements were necessary because of equipment malfunction, losses due to flooding and access difficulties in the upper reaches. However, almost complete data are available from the eight recording stations shown in Figure 4.15 for the period described.
2. Fifteen Odyssey Salinity and Temperature 0 to 80 mS cm^{-2} per centimetre data loggers were deployed at the same stations described in Figure 4.15, with the same restrictions as described above. The results from these loggers were

temperature corrected and converted to salinity units parts per thousand (ppt) using a conversion factor of 0.64. Latitude and longitude for these eight recording stations are shown in Table 4.4.

3. Hand-held hydrological recording devices included:
    a. a Hydrolab Quanta Water Quality Monitoring recorder, which was used for recording dissolved oxygen (mgl^{-1}), pH, temperature and salinity (temperature-corrected Practical Salinity Scale units)—this apparatus is very accurate but slow to stabilise, so for profile readings at varying depths this implement was supplemented by the instruments (b), (c) and (d),
    b. a YSI EC300 portable salinity conductivity, salinity and temperature meter,
    c. a PINPOINT II, PM025, High Performance Dissolved Oxygen Monitor,
    d. a PINPOINT PM001 pH Monitor.
4. Geographic instruments for topography measurements included:
    a. a Trimble 5800 RTK-GPS (Real Time Kinematic Global Positioning System),
    b. Lowrance Handheld GPS Model GO2,
    c. Bushnell Laser Rangefinder Model Sport 450.
5. Colorametric Chemical Analysis was conducted using a Palintest Comparator with analysis discs for aluminium, iron and sulphide ions.
6. Data for tidal flow rates were obtained from three sources:
    a. Slow flow rates below 0.2 ms^{-2} were obtained using a specially designed weighted float with a low wind resistance timed over a set distance.
    b. Other flow rates were measured using a propeller-based Global Water FP111 flow probe with a computer capable of true velocity averaging of a channel's flow.
    c. Longer term flow rate recordings were obtained using a Starflow 6526E21 Ultrasonic Doppler flow rate data logger.

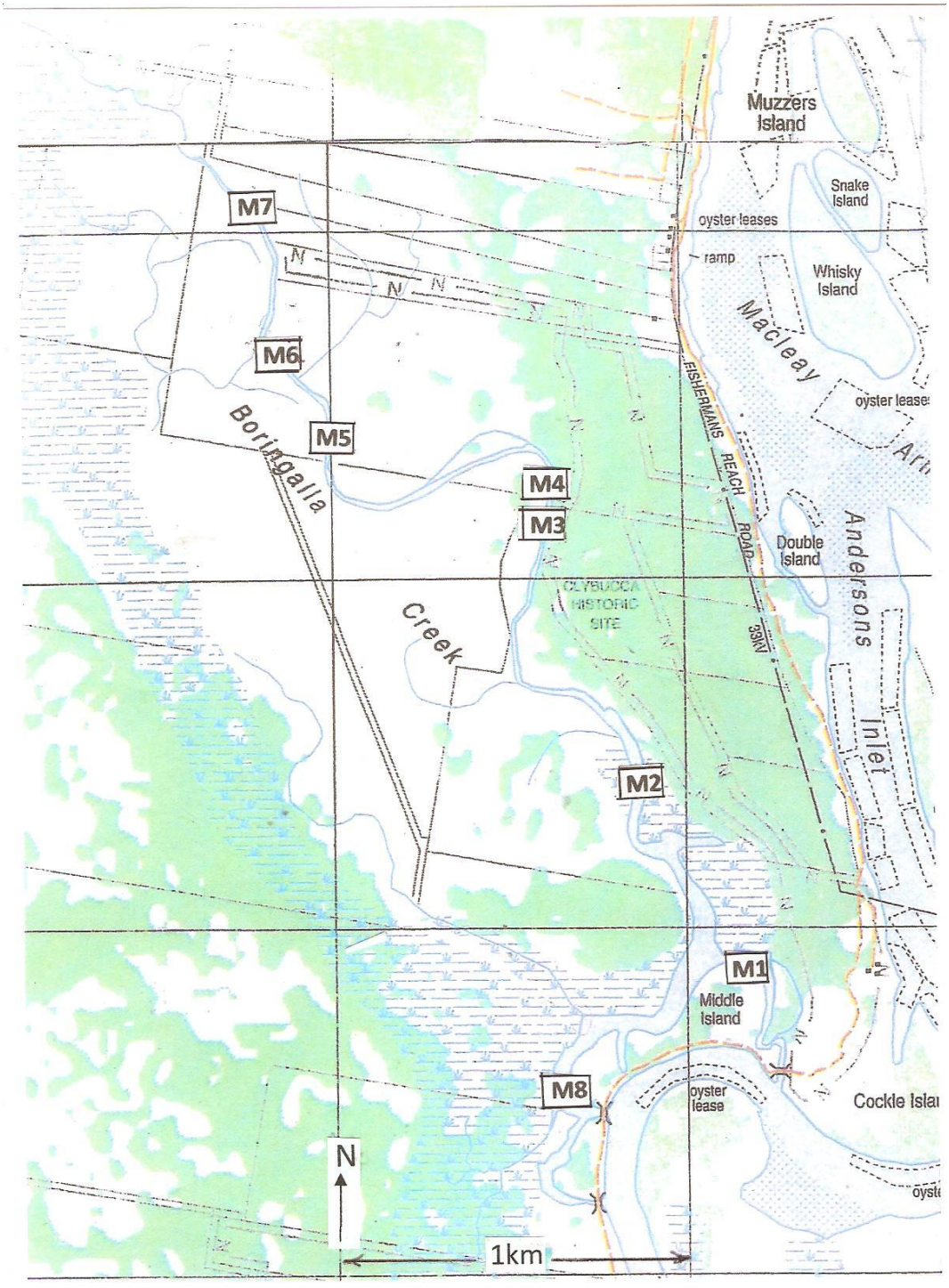

Figure 4.15: Positions of recording sites for data loggers

Table 4.4: Coordinates of data loggers

DATA LOGGER	LONGITUDE Degrees/Minutes	LATITUDE Degrees/Minutes
M1	152° 59.448’	30° 53.772’
M2	152° 59.275’	30° 53.470’
M3	152° 59.122’	30° 53.103’
M4	152° 59.132’	30° 53.053’
M5	152° 58.741’	30° 52.967’
M6	152° 58.674’	30° 52.854’
M7	152° 58.631’	30° 52.626’
M8	152° 59.133’	30° 54.002’
MHL	152° 57.698’	30° 51.498’

Other data were obtained from:

1. A water level data logger was installed by the MHL, funded by the DECC, in the upper reaches of the system, referred to as BORIRGALA CKCR8. This logger was commissioned in July 2008, has operated continuously with some short equipment losses caused by flooding and has the readings available online (position given in Table 4.4).
2. MHL, 2002–2012, NSW Tide Charts, NSW Department of Public Works and Services Publication, tidal data were supplied by MHL, NSW.
3. Australian Government BOM rainfall recording stations included:
   a. Station 5905 Eungai Creek (South Bank Road),
   b. Station 59068 Collombatti (Benbullen).
4. Glamore, W.C., Wasko, C.D. & Smith, G.P., 2012, Rehabilitation of Yarrahapinni Wetlands National Park: Hydrodynamic Modelling of Tidal Inundation, WRL Technical Report 2011/21, Water Research Laboratory, University of New South Wales, Manly.

4.5 Results

The results for the hydrology of the Yarrahapinni Wetland are presented in five sections:

1. the magnitude of the growth and decline of the infestation by *Phragmites australis* that causes internal connectivity fragmentation of the flow in the wetland,
2. the quality and quantity of the water external to the floodgate structure in the tributary, Andersons Inlet, available to enter the wetland,
3. the hydrological connectivity of tidal inflow that is controlled by the levy banks and floodgates structures and its effect on the physical and chemical hydrology of the wetland,
4. the hydrological connectivity to the upper freshwater wetland section that affects rainfall runoff and flooding.

4.5.1 Phragmites Australis

Once routine dredging ceased in Borirgalla Creek, the common reed (*Phragmites australis*) was able to propagate unchecked by first lining the bank regions and then spreading across the channel sections. By 2007, this creek was almost blocked at seven locations between 1 and 4 km from the floodgates, to the beginning of a 500-m long total blockage (Fig. 4.16).

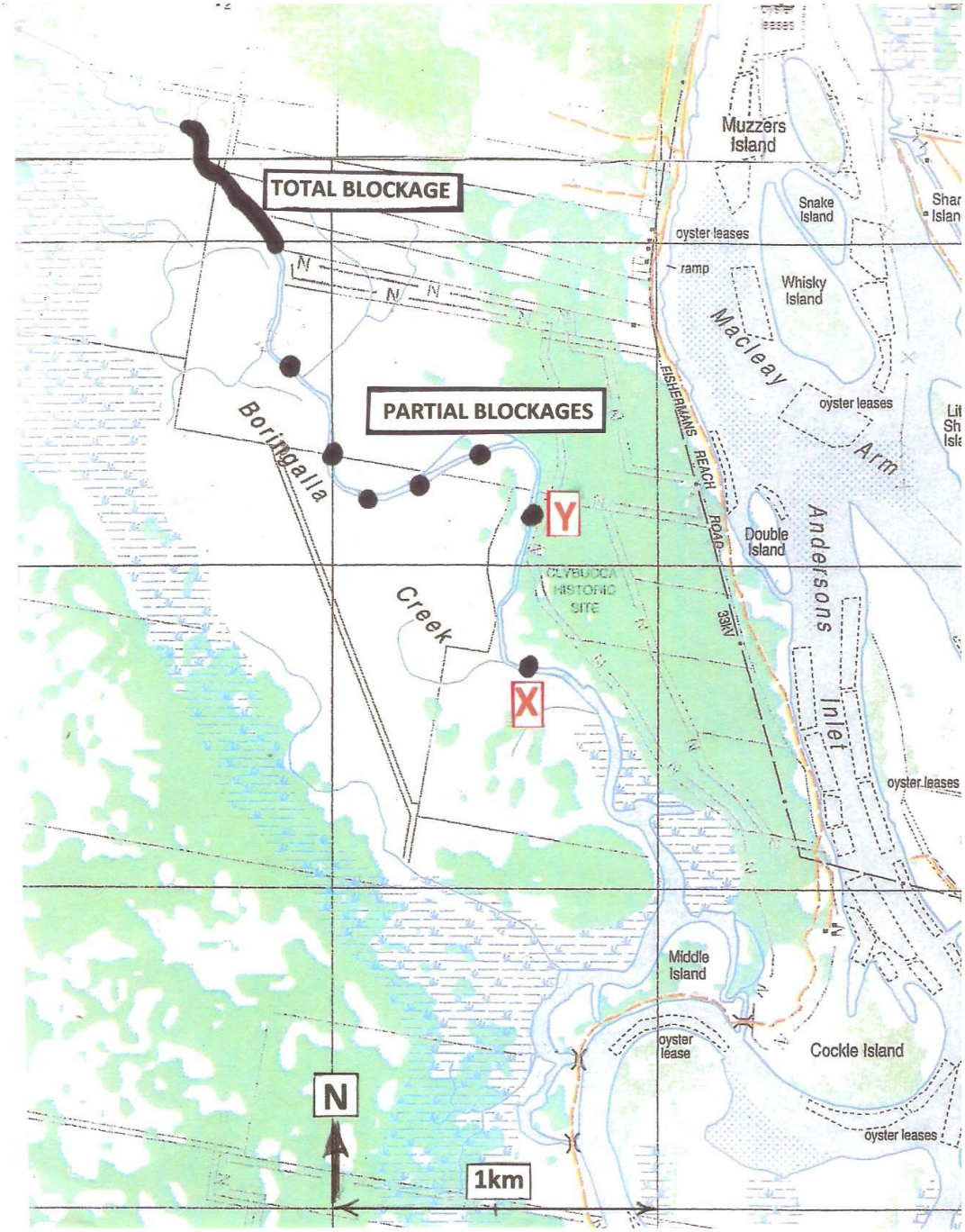

Figure 4.16: 2007 positions of *Phragmites australis* blockages (modified from LPI 2002)

These reed beds fragmented the hydrology of the creek; the small amount of salinity entered the lower wetland by leakage of the floodgates and levees and levee overtopping during very high tides, not penetrating far beyond the first blockage (X).

These blockages of *Phragmites australis* have changed considerably since 2007 because of the influence of increasing salinity within the wetland, which attacks this species (Chambers et al. 2003; Hellings & Gallagher 1992; Lissner & Schierup 1997).

These changes are the result of the increasing floodgate openings, but the effects have been gradual since 2007 and cannot be directly related to the floodgate-opening program.

In 2007, the first blockage—X in Figure 4.16—extended for approximately 50 m and was sufficiently dense to almost exclude flow and navigation (Fig. 4.17).

Figure 4.17: Blockage X on 25 November 2007

By November 2008, this bed had been eliminated, thus allowing the saline water to travel further upstream to blockage Y in Figure 4.16. Figure 4.12 shows the blockage at Y in November 2008, and Figure 4.18 shows the same blockage in November 2012.

(a)

(b)

Figure 4.18: (a) Phragmites blockage at Y, November 2008 (note position of PVC pipe for water level data logger), (b) position of blockage Y, November 2012, with the same (discoloured) PVC pipe

With phragmites blockages X and Y removed, the increasing upstream salinity has also significantly reduced to the six minor phragmites blockages upstream of Y (Fig.4.16).

Figure 4.19 shows the 'total blockage' referred to in Figure 4.16.

Figure 4.19: Start of the total blockage, November 2008

This blockage has not changed to any significant extent since 2007. It is impenetrable and extends for approximately 600 m, and indications are that there has been significant siltation within the reeds because there is no hydrological connectivity through this bed, in either direction. Freshwater runoff from the upper region travels over the eastern bank, and there is no indication of any tidal or salinity influence above the blockage.

On 3 August 2011, a field survey of depth profiles within the Yarrahapinni Wetland was performed, using a Trimble three-dimensional GPS, in cooperation with the staff of the Water Research Laboratories, UNSW. The positions of the depth transects are shown in Figure 4.20, and the resulting profiles are shown in Figures 4.21 (a) and (b). The

results for positions 7, 8 and 9 are excluded because of difficulties caused by overhanging vegetation interfering with the recording signal in the narrow creek sections.

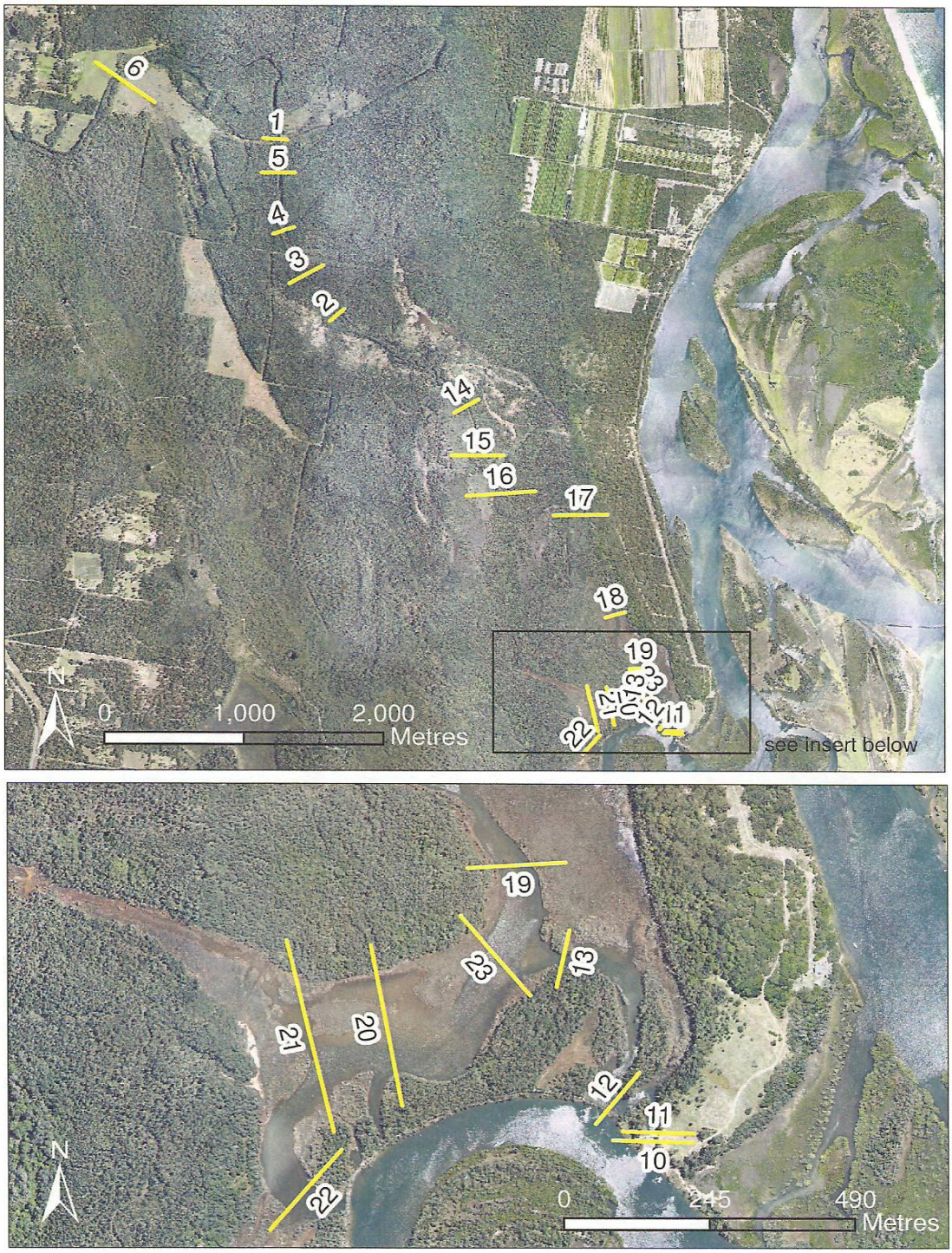

Figure 4.20: Positions of depth profiles (Glamore et al. 2012)

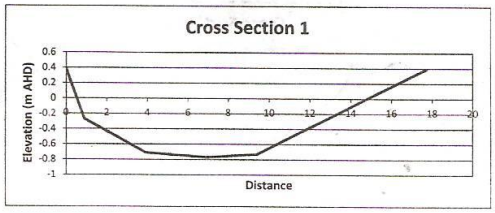
Cross Section 1
Elevation (m AHD)
Distance

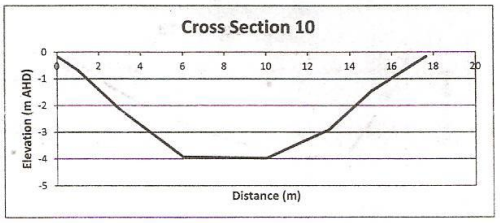
Cross Section 10
Elevation (m AHD)
Distance (m)

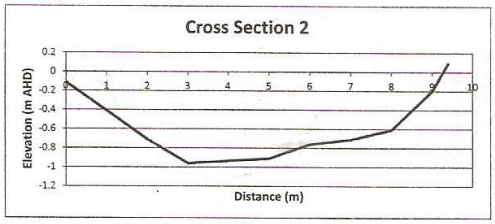
Cross Section 2
Elevation (m AHD)
Distance (m)

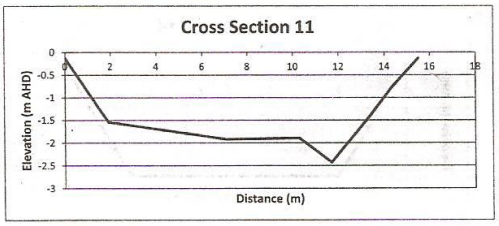
Cross Section 11
Elevation (m AHD)
Distance (m)

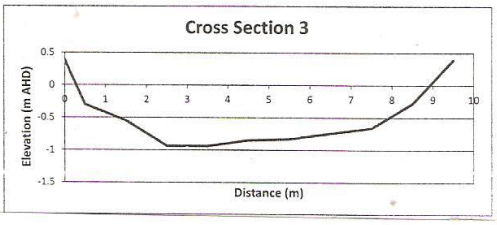
Cross Section 3
Elevation (m AHD)
Distance (m)

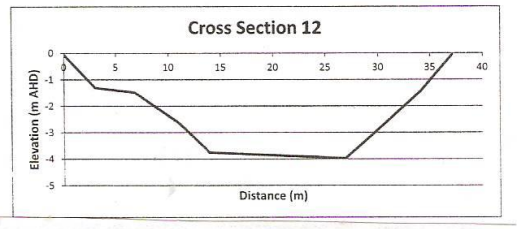
Cross Section 12
Elevation (m AHD)
Distance (m)

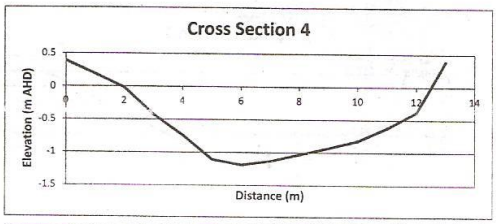
Cross Section 4
Elevation (m AHD)
Distance (m)

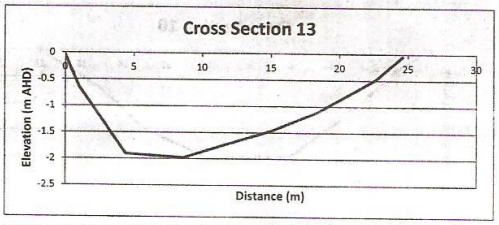
Cross Section 13
Elevation (m AHD)
Distance (m)

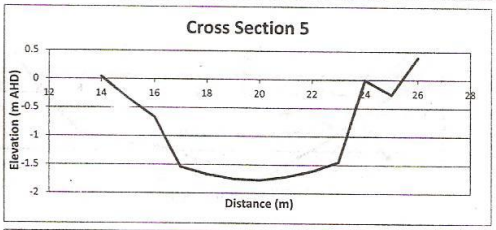
Cross Section 5
Elevation (m AHD)
Distance (m)

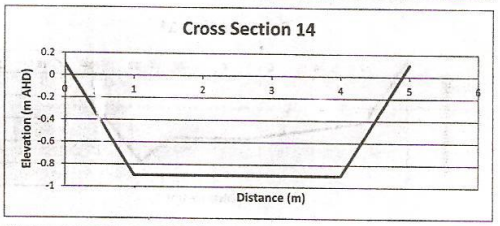
Cross Section 14
Elevation (m AHD)
Distance (m)

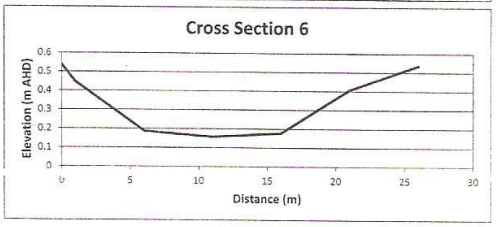
Cross Section 6
Elevation (m AHD)
Distance (m)

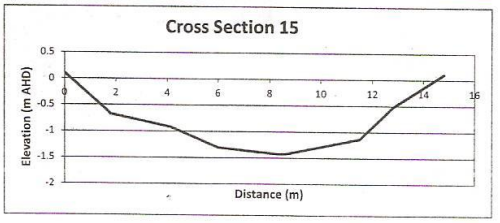
Cross Section 15
Elevation (m AHD)
Distance (m)

(a)

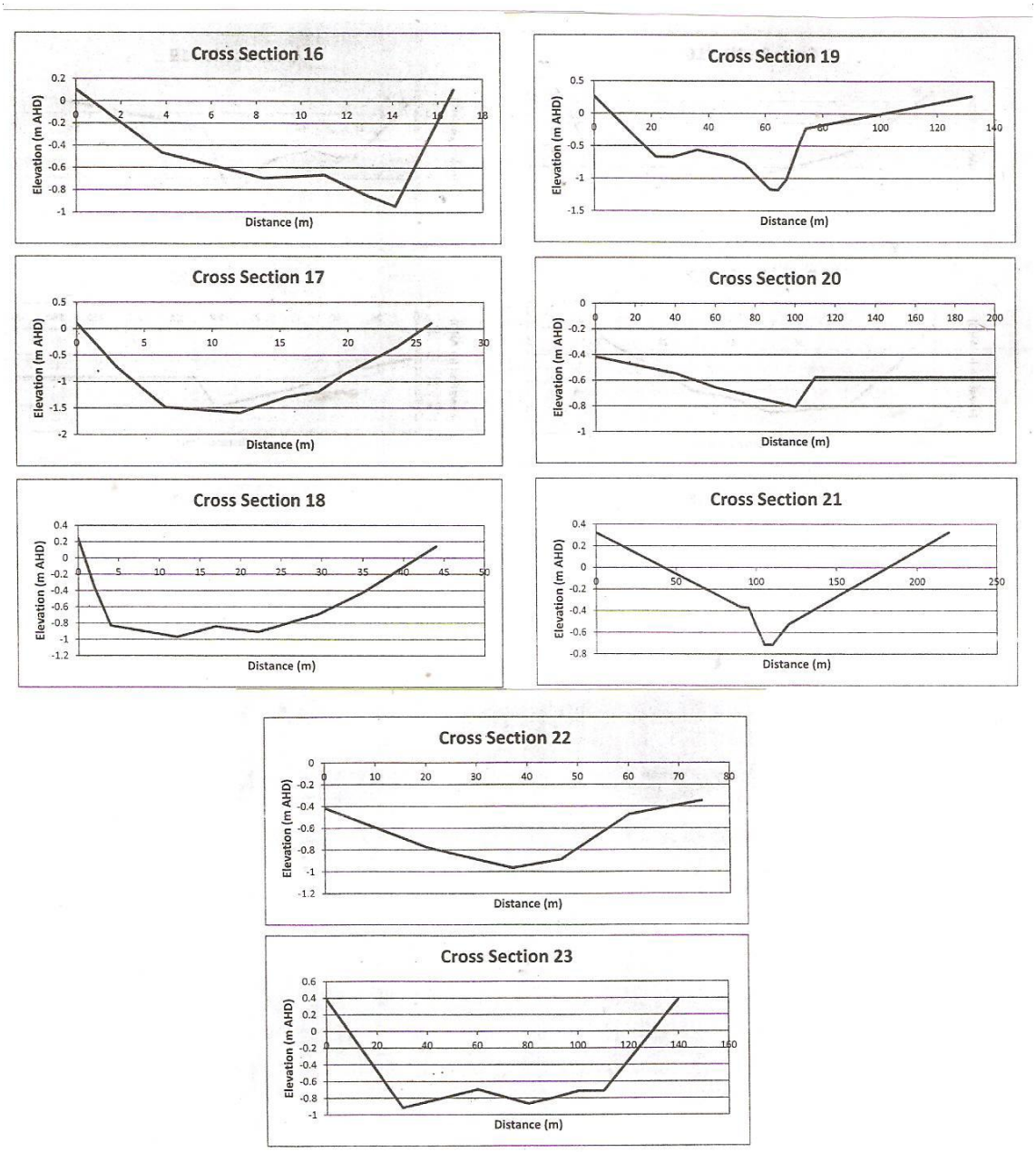

(b)

Figure 4.21: The depth profiles for the positions shown in Figure 4.20 (Glamore et al. 2011)

These results, changing reed beds and direct observations indicate that the wetland has become a system with three distinct zones of varying morphology and hydrology (Fig. 4.22):

- Zone A: the faster-flowing, deeper tidal creek, which follows the path of the original Borirgalla Creek up to the total phragmites blockage,

- Zone B: the low-velocity, shallow areas that were known as the Broadwater and Middle Creek, which also now includes the shallow areas formed when the incoming tidal levels overtop the creek banks of Zone A and penetrate large areas of the surrounding vegetation,

- Zone C: the freshwater, non-tidal lagoon upstream from the total blockage, which can extend 500 m on either side of the original dredged creek following periods of high rainfall.

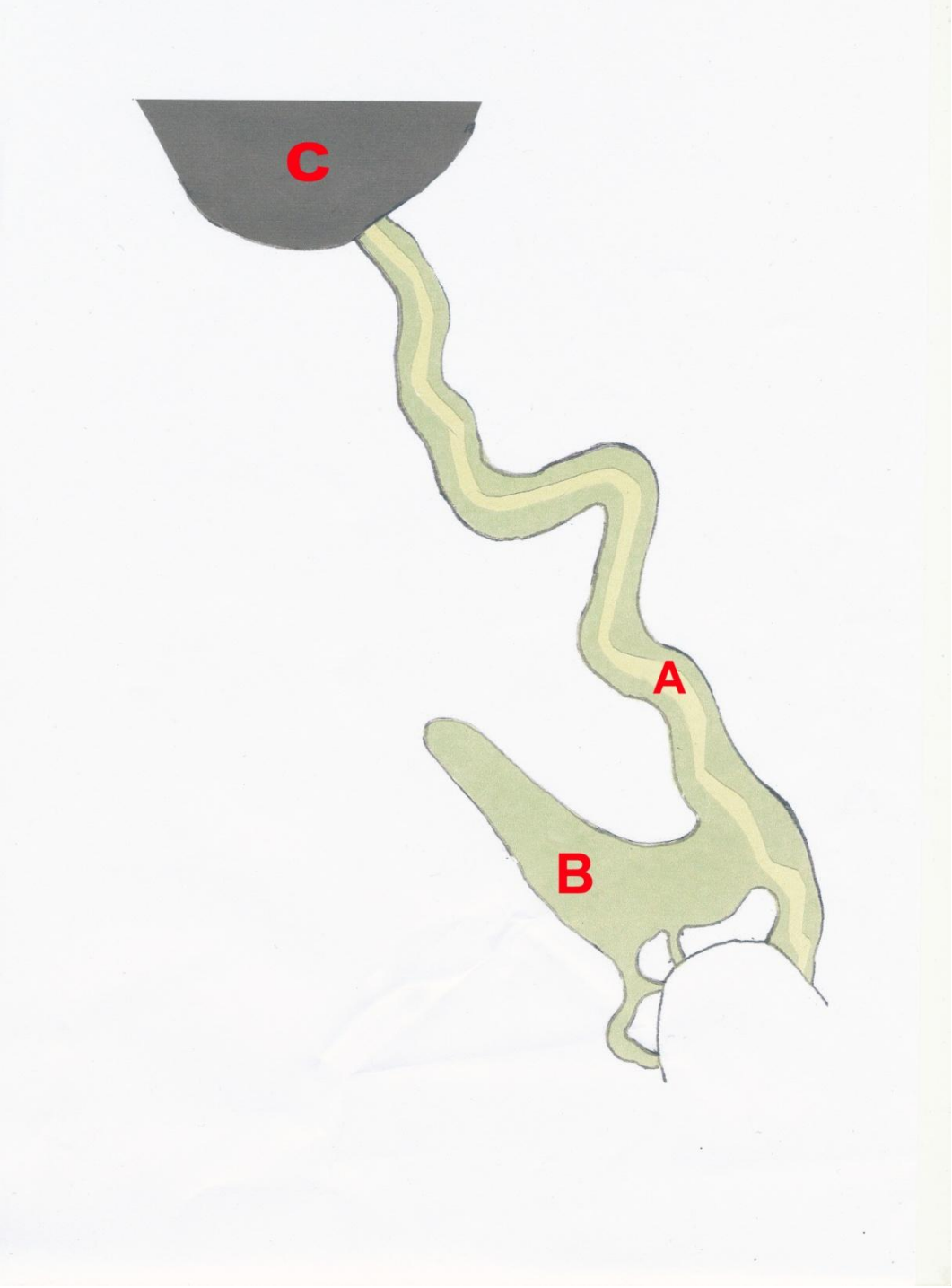

Figure 4.22: Schematic representation of the areas of the three distinct zones

4.5.2 Quality and Quantity of Water External to the Floodgates

The quality of the water external to the floodgates is a complex balance between incoming seawater and outflow from the Clybucca wetland, discharging into Andersons Inlet. This aspect of the hydrology of Andersons Inlet is investigated in Chapter 5.

4.5.3 Hydrological Connectivity at the Floodgates

(Note: The results in this subsection have been chosen from a large volume of data obtained from the array of Odyssey data loggers, to illustrate the effects of inflowing estuarine water. To this end, the results shown are from data obtained when there had been no significant rainfall in the wetland catchment for at least 25 days so that the results reflect the effects of only incoming tidal influences.)

The hydrological conditions within the Yarrahapinni Wetland varied considerably with various stages of hydrological connectivity.

STAGE 2

From 4 December 2007 to 5 February 2010

Hydrological connectivity: 4%

The water levels for a 14-day period in January 2010 at the logger station M1 are shown in Figure 4.23. The tidal pattern at this stage has not achieved the conventional sinusoidal pattern for an estuary because the tidal range within the wetland is controlled by the small openings.

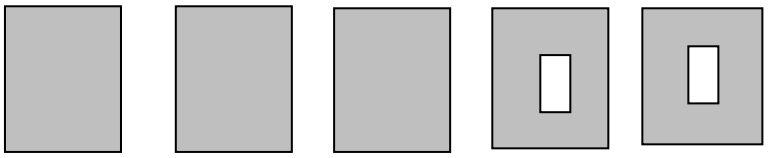

(a)

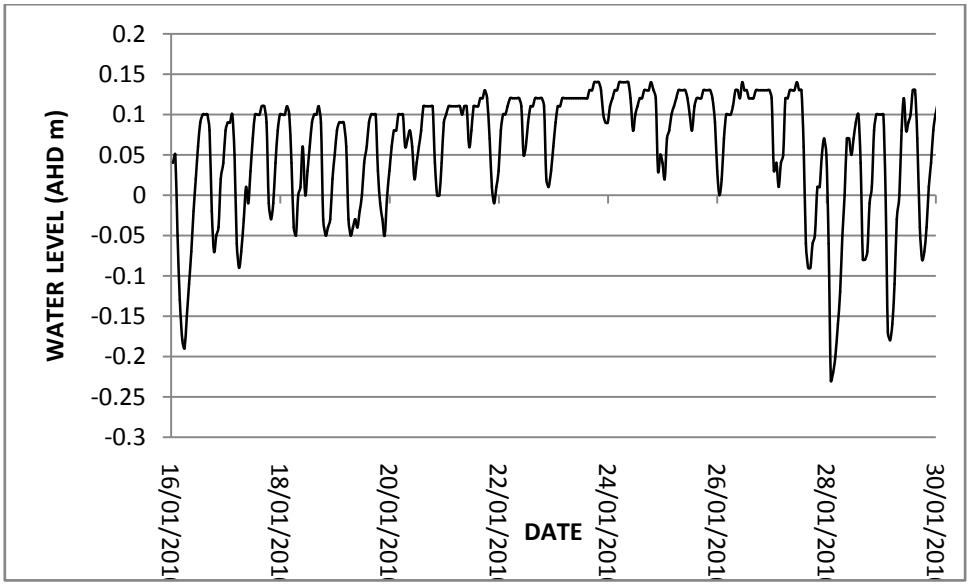

(b)

Figure 4.23: (a) Schematic drawing of floodgate openings, (b) water levels at Site M1 for a 14-day period commencing 16 January 2010

STAGE 3

From 5 February 2010 to 24 July 2011

Hydrological conductivity 24%

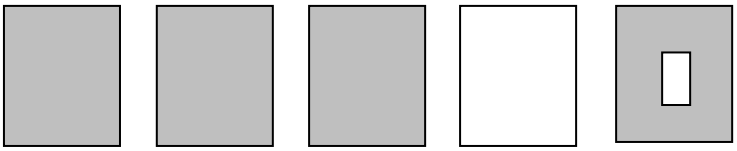

(a)

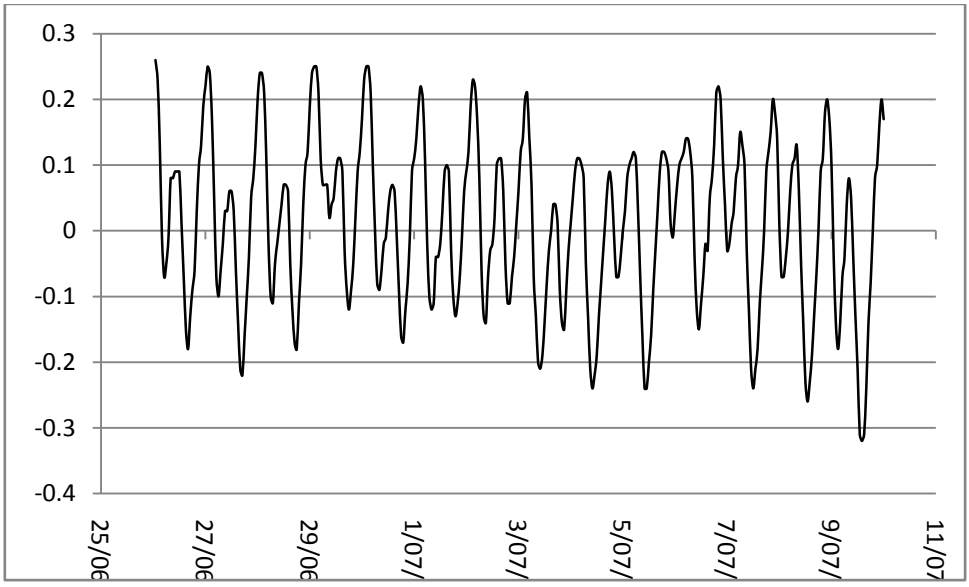

(b)

Figure 4.24: (a) Schematic diagram of floodgate openings, (b) water levels at Site M1 for a 14-day period commencing 26 June 2010

STAGE 4

Commencing 24 July 2010

Hydrological connectivity 63%

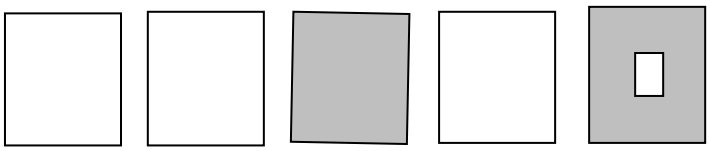

(a)

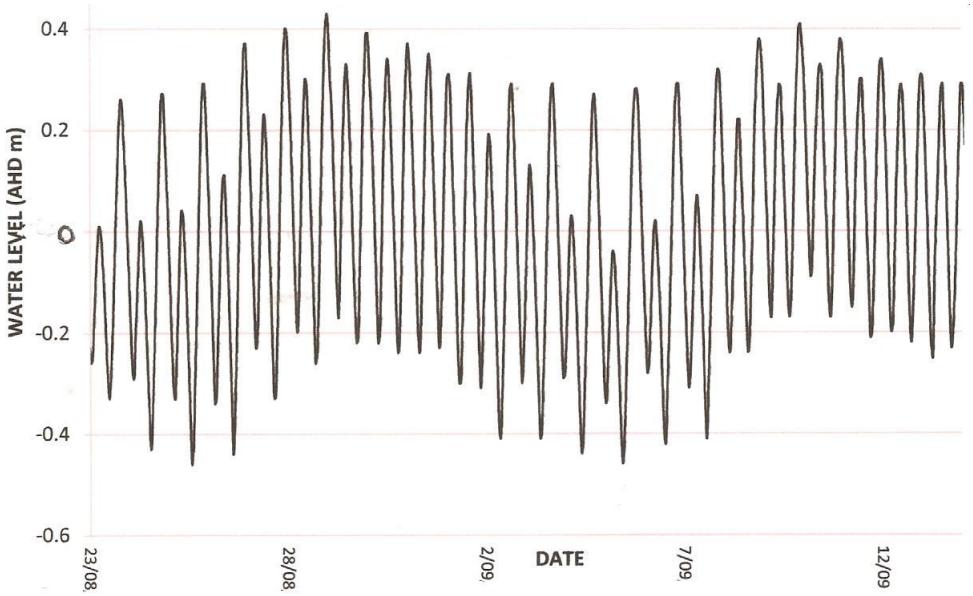

(b)

Figure 4.25: (a) Schematic diagram of floodgate openings, (b) water levels at Site M1 for a 21-day period commencing 23 August 2011

Results of examples of the water level changes that occurred during these four stages can be compared by compacting Figures 4.10, 4.23 (b), 4.24 (b) and 4.25 (b) and presenting them on a single diagram (Fig. 4.26). This diagram shows that mean tidal level of approximately 0 AHD and a conventional sinusoidal tidal cycle were not achieved until Stage 3 (connectivity 24%).

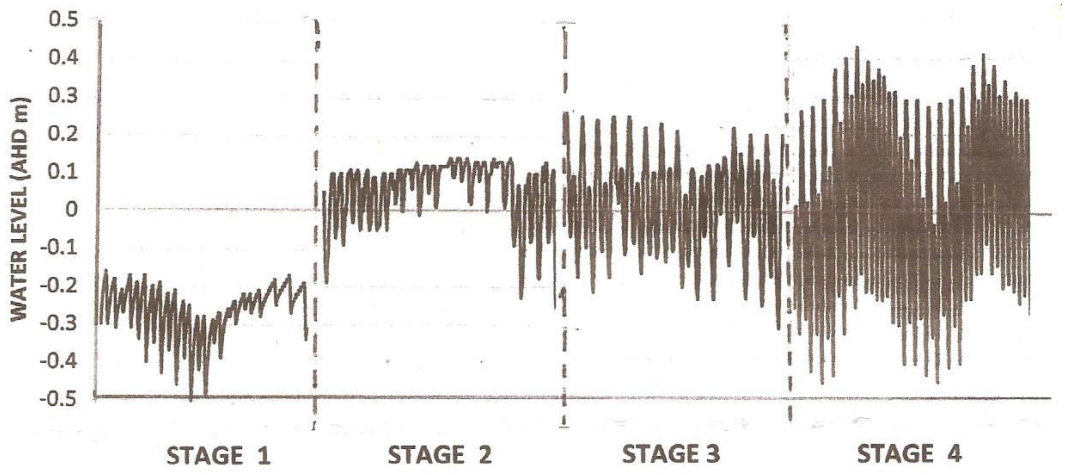

Figure 4.26: Change in tidal range and mean water levels for four stages (mean water level for Stage 1 approx. –0.3 AHD; MHL2004)

The typical tidal ranges achieved for the four stages are compared with the connectivity of these stages in Figure 4.27.

(The use of fluid dynamics computer models for tidal situations was far outside the budget restraints of this thesis study)

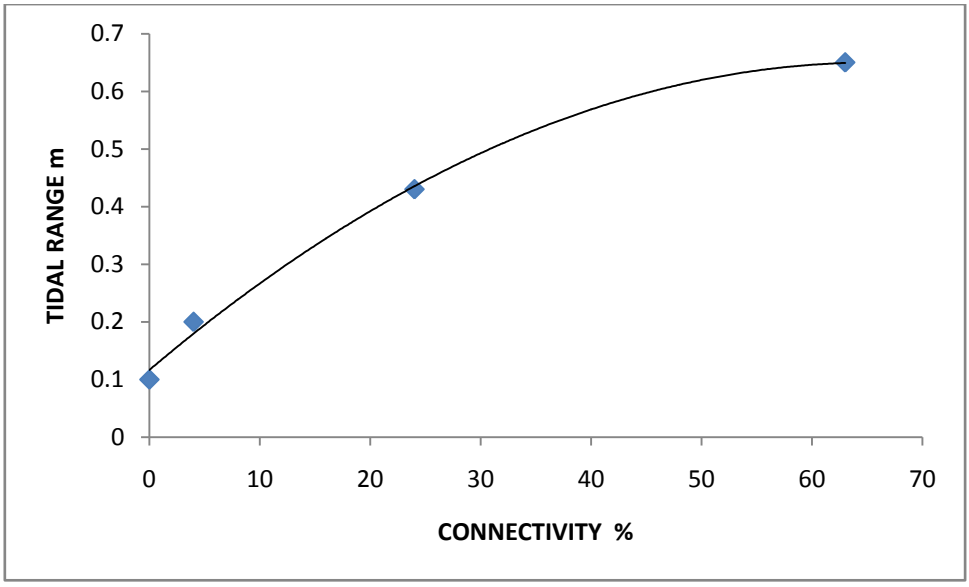

Figure 4.27: Tidal ranges for the four stages compared with connectivity

Figure 4.27 shows that the rate of influence on the tidal range of increasing connectivity diminishes with increasing connectivity.

It was not possible to compare complete tidal prisms within the wetland for the differing floodgate configurations because increasing water heights overtopped the creek banks. This meant that, at varying times in the tidal inflow, the area of flow would start to increase as the tide flowed through the vegetated creek banks. The satisfactory alternative is to compare the tidal flows for the incoming tide early in the tidal cycle when the maximum flow rate has been reached and the flow is still contained within the creek banks (Table 4.5).

Table 4.5: Maximum incoming flow rates compared with percentage hydrological connectivity at the floodgates

STAGE	CONNECTIVITY %	DATE	FLOW RATE m^3/sec
1	0	N/A	0
2	4	16/12/2009	1.9
3	24	9/8/2010	7.9
4	63	3/11/2012	11.8

The results from Table 4.5 are shown graphically in Figure 4.29:

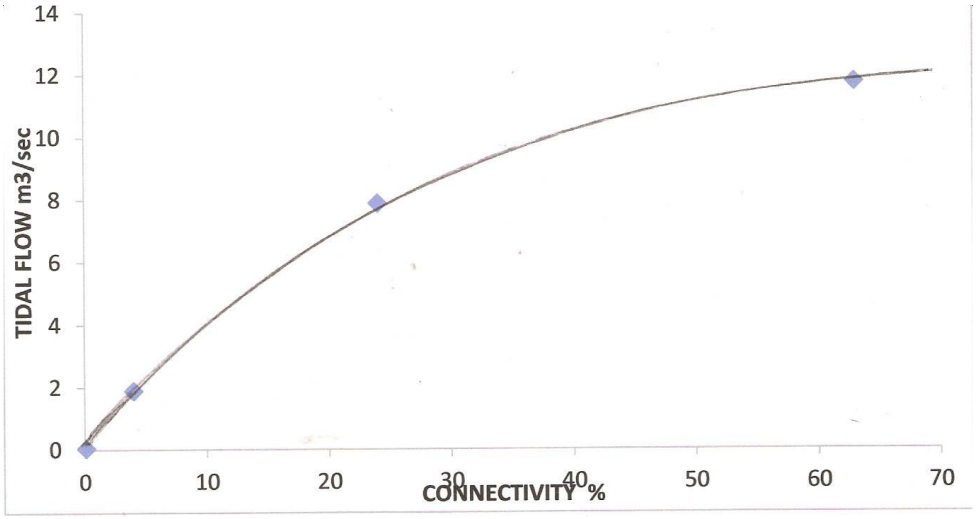

Figure 4.28: Comparison of hydrological connectivity and maximum flow rates within the wetland

Figure 4.28 again shows the diminishing effects of increasing connectivity, which may be explained in terms of diminishing driving force across the floodgate system.

Increasing connectivity throughout the trial period led to a reduction of the phragmites fragmentation and improved the tidal flow in the upper regions of the system. Figure 4.30 shows the tidal range during the different stages at recording station M5 (Fig.

4.15). This graph shows that a conventional sinusoidal waveform with a significant tidal range was not achieved in the upper reaches of the system until Stage 4 of the trial.

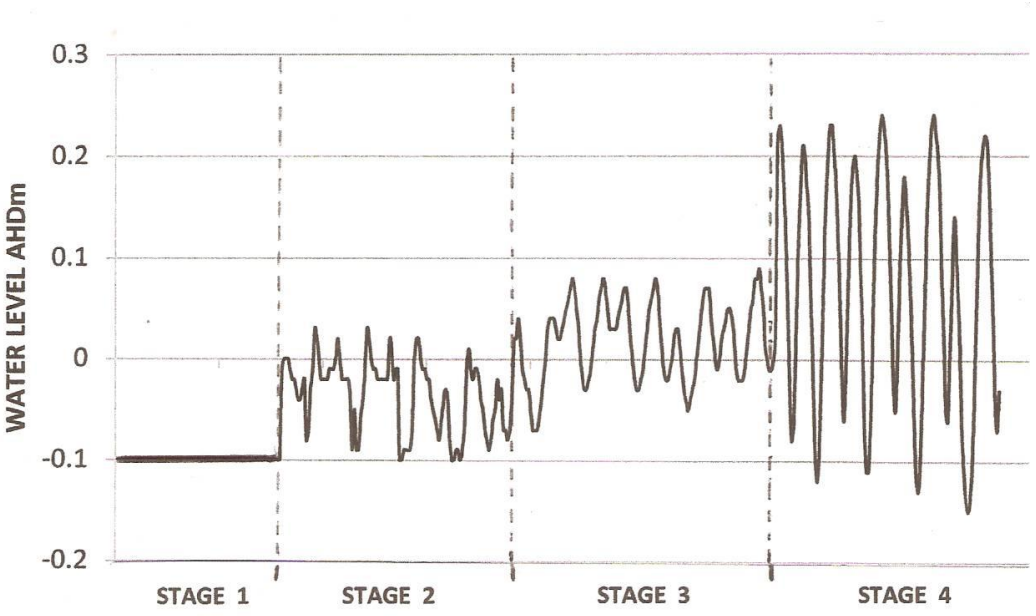

Figure 4.29: Tidal ranges during the four stages at recording station M5

The distribution of salinity within the wetland system was examined to determine the effects of the changing phragmites beds. Figure 4.30 shows salinity readings recorded on 12 May 2008 using the 'moving boat method' (Savenije 2005).

This method involves following the high-water tidal wave throughout the length of the waterway, recording salinity profiles with a hand-held salinity meter during a period with minimal runoff of fresh water.

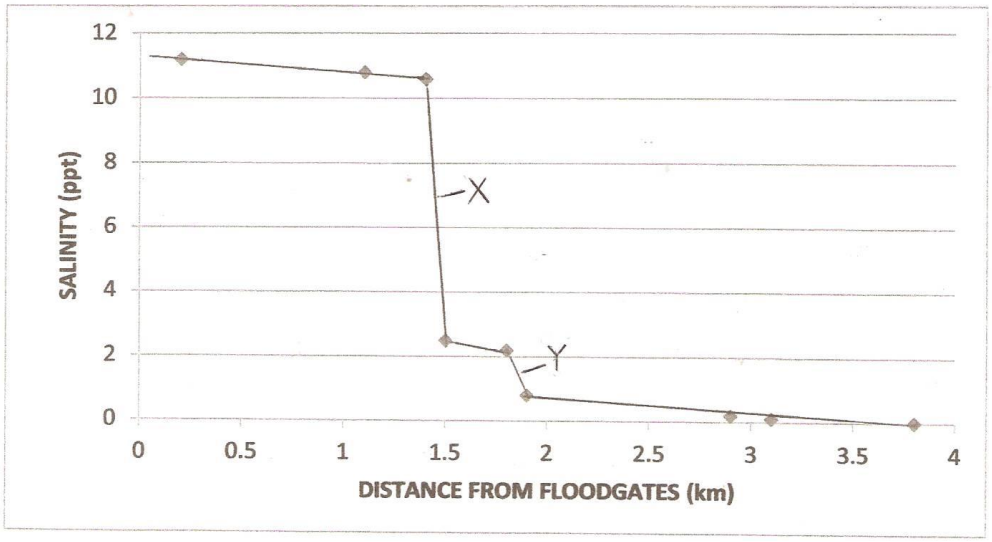

Figure 4.30: Salinity of wetland compared with distance from floodgates, 12 May 2008

Sharp decreases in salinity occur across phragmites beds X and Y as indicated.

The reed bed at X had not diminished to any great extent in May 2008, as indicated in Figure 4.30, but was eliminated by November that year.

A similar salinity survey was performed on 11 November 2012, and the results represented in Figure 4.31 show that the phragmites beds no longer influence the hydrology of the lower section of the system.

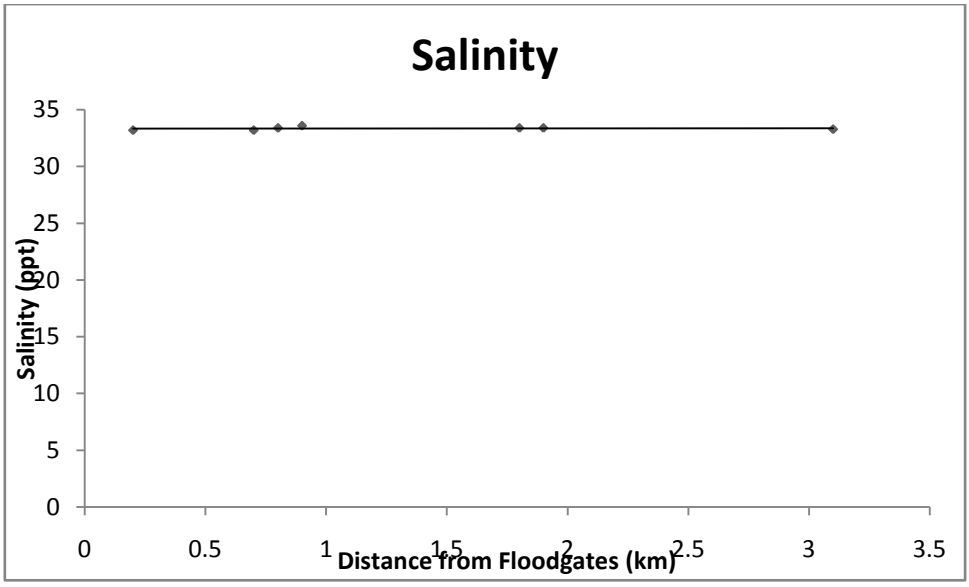

Figure 4.31: Salinity compared with distance upstream from floodgates 11 November 2012

4.5.4. Influence of the Upstream Freshwater Wetland Section

A large freshwater region in the upper reaches has been present since the floodgate opening trial commenced in 2007. This section was formed by the regrowth of phragmites since routine creek dredging finished in 1996. Following heavy rainfall, the blockage acts as a dam, resulting in a very large lake forming over the creek banks and slowing the runoff process. The depth of this lake has been monitored throughout the trial by the MHL water level logger, approximately 1.5 km upstream from the start of the blockage. Figure 4.32 shows a comparison of the readings from this logger with the rainfall figures from the BOM Eungai station for a five-month period during 2009, showing two flooding events and a recovery period.

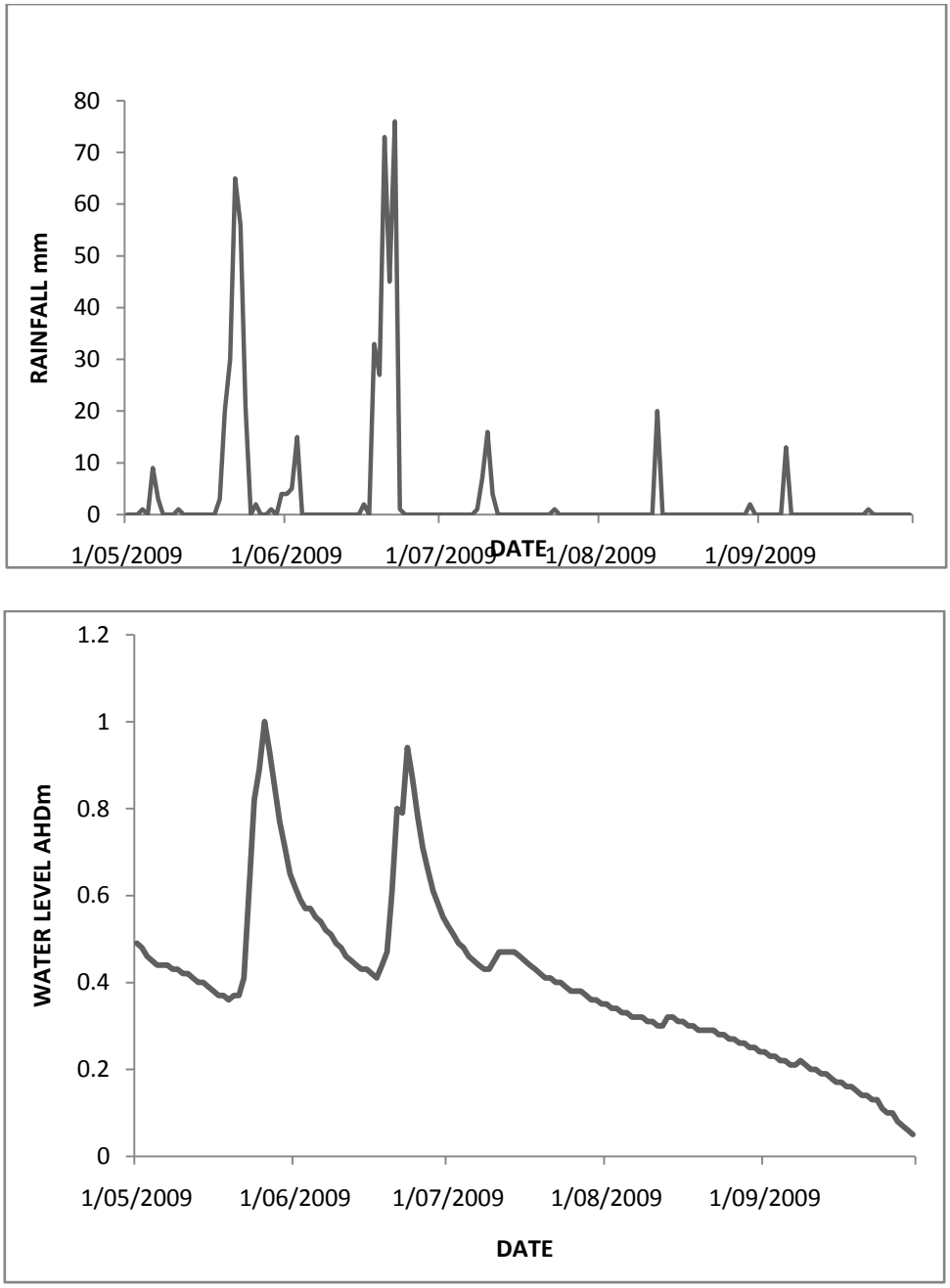

Figure 4.32: Comparison of water level height and rainfall for the freshwater region

There is a very close correlation between the rainfall and the water level in the freshwater region, as shown in Figure 4.32. The two flood peaks are evident, with an approximately three-day delay, as are the three minor rainfall events following the second flood. This graph also shows that recovery from heavy rainfall is very slow

because of the damming effect of the blockage with the region, taking three months to return to its original level.

The effects on the water chemistry of the wetland of the balance between the incoming tidal cycle and the flooding–recovery cycle of freshwater discharge from the upper region were also examined. Figure 4.33 shows the daily readings from the water level data logger at the upper MHL recording site for a period from November 2011 to April 2012. This can be compared with the hourly salinity readings from the data logger at the recording site M1 for the same period (Fig. 4.34). These figures illustrate the following points:

1. There is a very close relationship between water level height within this freshwater region and the effect on the salinity within the wetland system.
2. The salinity within the wetland experiences a continual cycle of rapid decreases because of rainfall events followed by recovery to original levels, as shown by the eight such cycles, of varying magnitude, in a five-month period.
3. Salinity ranges after the two major flooding events in November 2011 and February 2012 were very small for a short period. The salinity levels in the wetland were re-established during the top of the tidal cycles but subjugated by the stronger flooding runoff during the rest of the tidal cycle.
4. Salinity levels during the six minor runoff events suffered a lower decrease in range and a smaller variation in salinity during a tidal cycle, depending on the magnitude of the event.

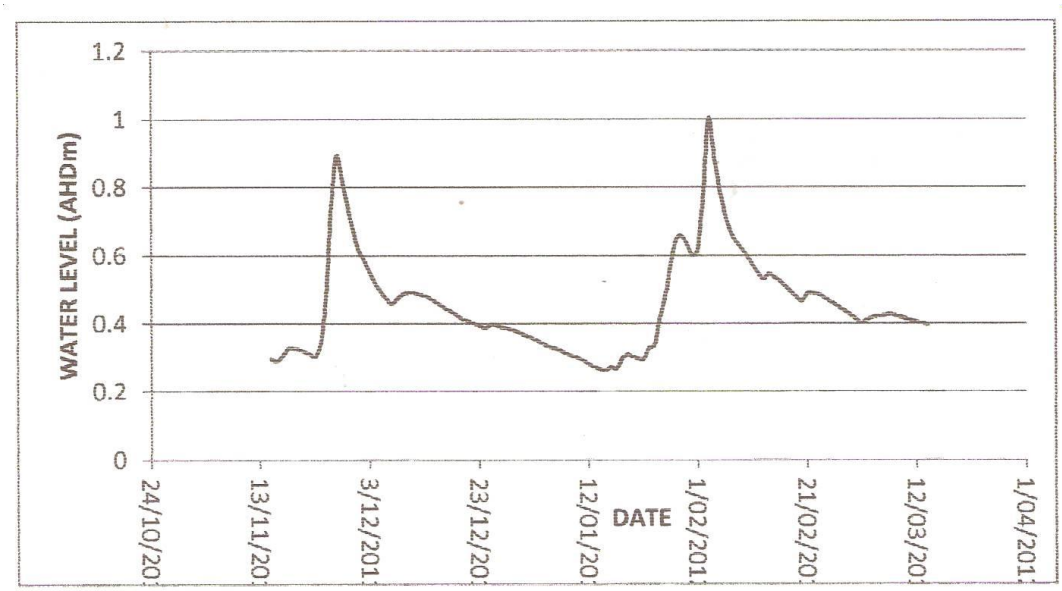

Figure 4.33: Water level heights from the MHL logger in the freshwater region

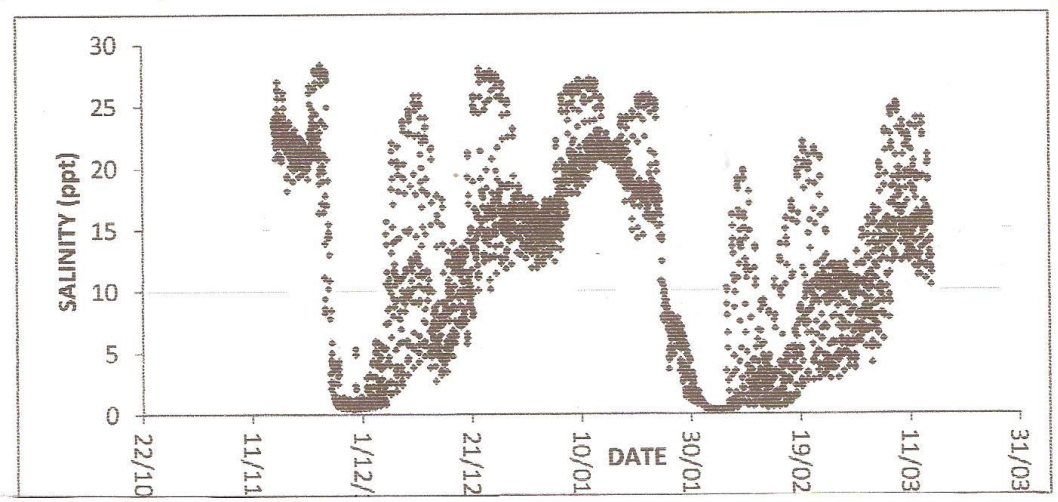

Figure 4.34: Hourly salinity readings from the data logger at M1 for the same period as Figure 4.35

A more detailed record of the salinity recovery following a major flooding event is presented in Figure 4.35, which shows the hourly salinity recordings at recording station M1 for the period from 16 October 2011 to 15 November 2011.

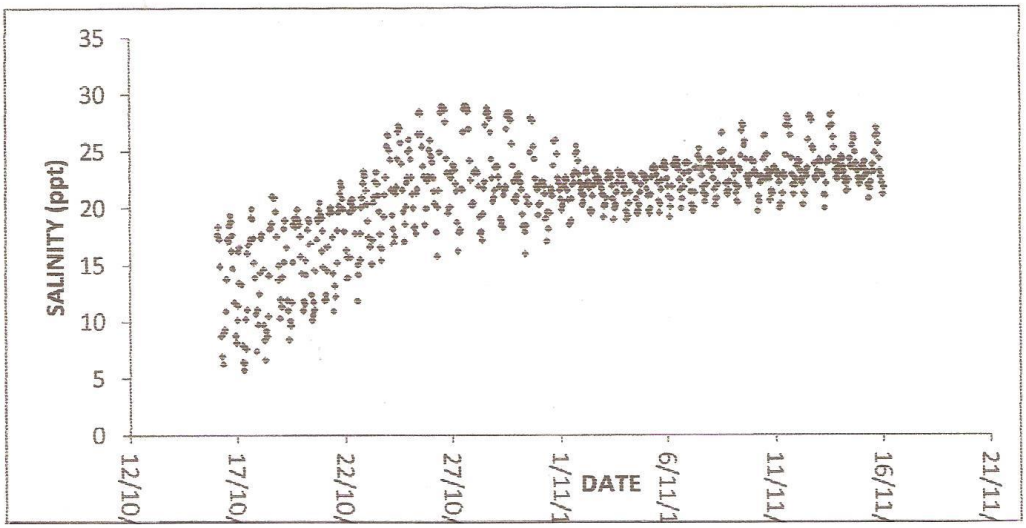

Figure 4.35: Hourly salinity recorded at M1 for a 31-day period 2012

Figure 4.35 again shows the range of salinity during the salinity recovery process. By choosing the lowest salinity for each tidal cycle in this period, it is possible to eliminate the temporary penetration upstream of higher salinities of the incoming high tides (Fig. 4.36). The resulting curve indicates a close correlation with a logarithmic function.

The correlation between the water level of the freshwater section of the wetland and its recovery of salinity can again be shown by comparing Figure 4.36 with Figure 4.37, which shows freshwater levels for the same period.

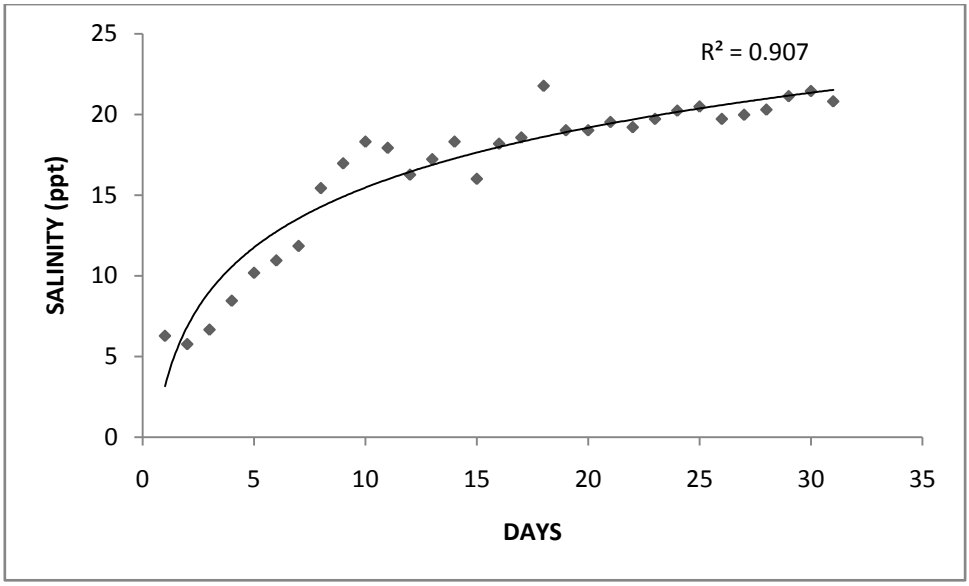

Figure 4.36: Logarithmic relationship between wetland salinity and time of recovery

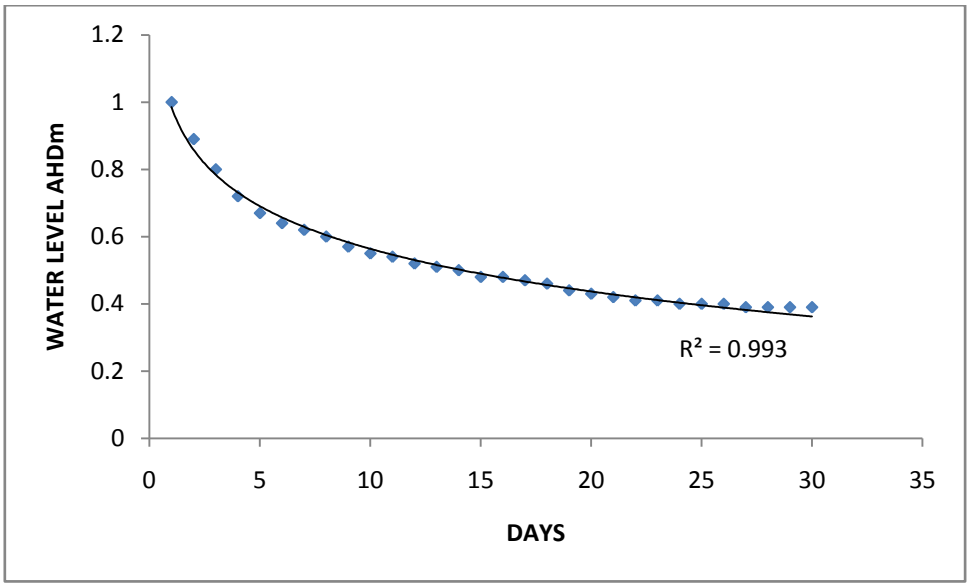

Figure 4.37: Logarithmic relationship between freshwater water levels and time of recovery of salinity

This curve also illustrates the pattern of discharge of floodwaters from the freshwater section of the wetland, confirming the lack of connectivity in the creek section because of the phragmites blockage and the slow method of discharge across the eastern creek bank region. A comparison of a flood event discharge pattern from Stage 2 (May 2009) with a similar event from Stage 4 (February 2012) shows that this discharge pattern

has changed during the opening trial (Fig. 4.38). This decrease in discharge rate possibly shows the increasing loss in connectivity through the phragmites blockage by increasing siltation within the reed bed during the trial period.

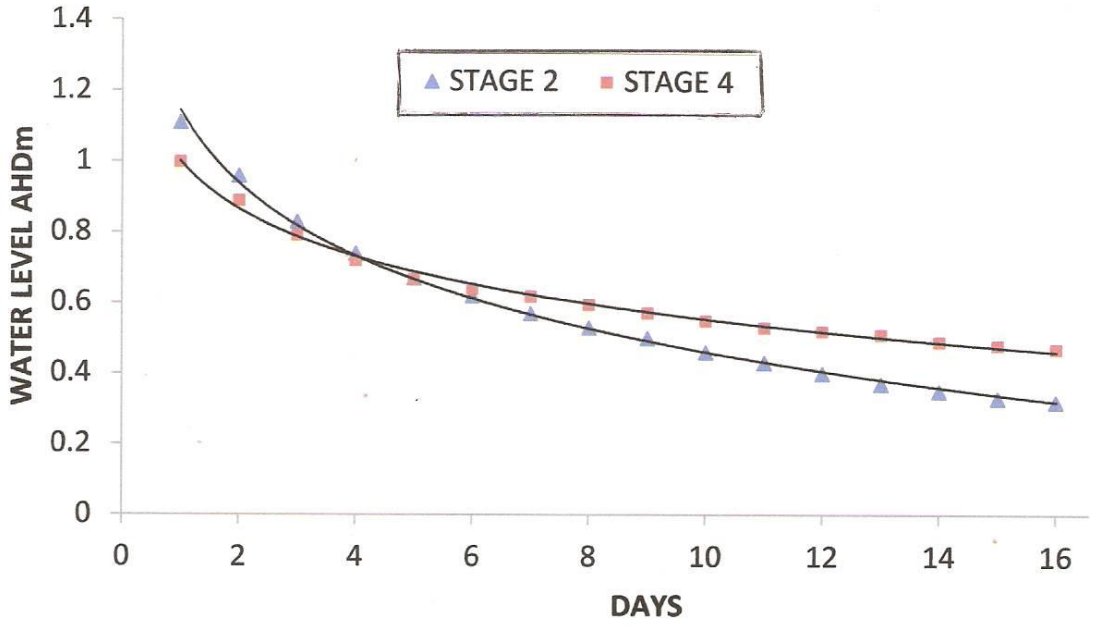

Figure 4.38: Freshwater discharge curves for Stages 2 and 4

The pH of the wetland system was found to have a close correlation with the salinity, so it is also controlled by the wetland section. The water quality survey performed by the MHL from 5 April to 27 September 2001 included data for salinity and pH at the recording station referred to as M1 in this study (MHL 2002). These data show that there are two regions of high correlation between the pH and the salinity at M1. The region below pH 7 is when the freshwater section is dominant, and the region above pH 7 shows the typical ocean water correlation (Fig. 4.39).

A similar comparison of pH and salinity for the period from 2008 to 2012 during the trial openings is shown in Figure 4.40. During the 2007 to 2012 trial period, the possibility of an acid sulfate discharge was always an important consideration, so a much larger number of the routine boat water tests occurred following periods of rainfall, and particularly following flooding events. As a result, a very large proportion

of the readings for Figure 4.39 fall in a very small region of the graph at pH values less than 2 and pH readings between 5.2 and 6. For clarity, this group of results has been excluded.

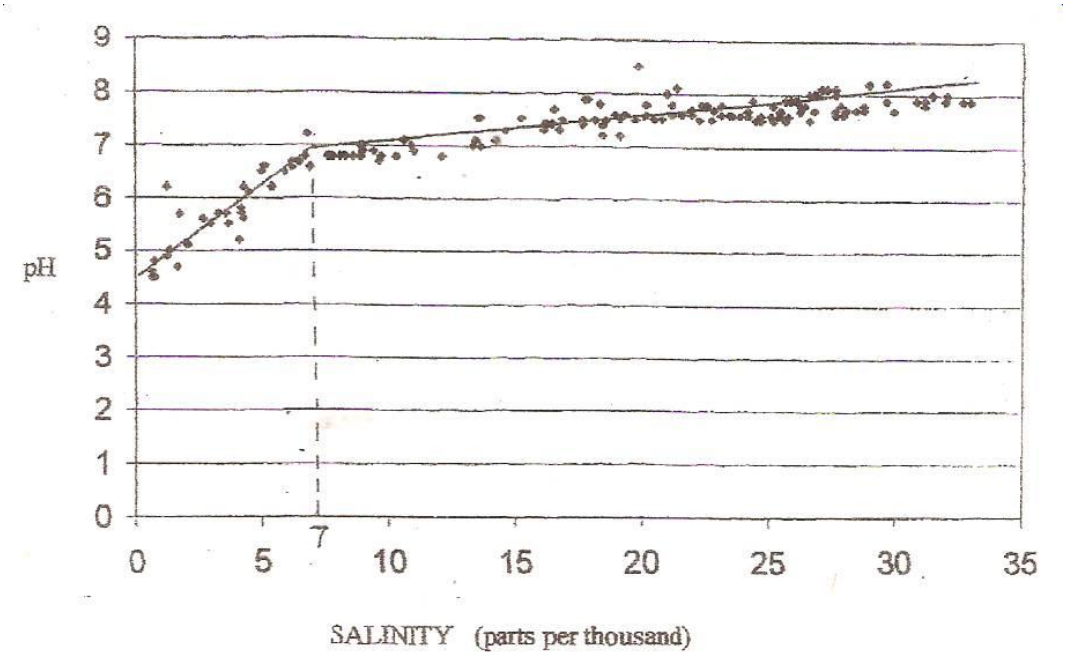

Figure 4.39: Comparison of pH and Salinity, April–September 1996 (MHL 2001)

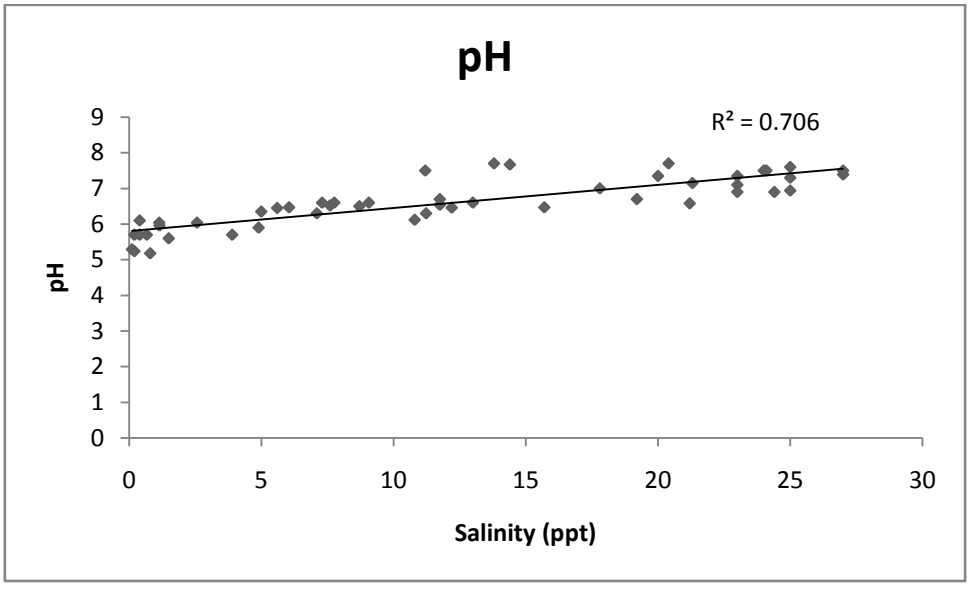

Figure 4.40: Comparison of pH and salinity, 2008–2012

The lowest pH reading encountered within the wetland during the trial period was 5.18, recorded at monitoring site M4 on 12 May 2008. This reading was taken in the upper reaches of the wetland in the early stages of the trial when the connectivity with the upper reaches was low. There were no other signs of an acid sulfate event elsewhere in the system. This would indicate that there has been no significant acid sulfate event within the wetland since the trial started in December 2007.

Other monitoring of water quality variables occurred during the study period with the purpose of detecting deleterious acid sulfate effects. These included dissolved oxygen content testing (from a boat), and taking samples for land-based colourimetry testing for aluminium, iron and sulphide ions, particularly during 2009 to 2011. The difficulty with the testing for acid sulfate effects is that their occurrence is spasmodic, only developing during a long dry period for oxidation to occur followed by a flooding event discharging the acid material in one event (Cook et al. 2000; Dawson 2002; Sammut et al. 1995). Such a set of conditions occurred in February 2009, November 2009, November 2010 and December 2011, but no acid sulfate conditions reached a level able to be registered on the recording equipment (Table 4.6).

Table 4.6: Highest levels of recorded ion contents

ION TESTED	Highest Level Recorded
Aluminium	> 0.05 mg/L
Iron	> 0.02 mg/L
Sulphide	> 0.05 mg/L

An acid sulfate event was detected in 2007 before the trial opening started. Most of 2007 experienced below-average rainfall until 256 mm was recorded at the BOM Station 59075 in the wetland catchment on 20 and 21 August. The water quality testing on 29 August at station M1 gave readings of salinity 0.05 ppt, pH 4.47, and dissolved oxygen 3.1 mg/L. There was considerable evidence of a 'fish kill': many bodies of *Acanthopagrus australis* (bream), *Sillago ciliata* (whiting) *and Mugil cephalus*

(mullet) were observed floating on the surface. There were also many examples of mullet swimming on the surface in an almost vertical position with their heads out of the water in an attempt to increase the intake of oxygen into their gills. No such occurrence of a 'fish kill' has been observed since the opening trial began in December 2007.

4.6 Summary and Discussion

The results of this study led to the following observations and conclusions:

1. Once routine maintenance dredging of the Borirgalla Creek ceased, the Yarrahapinni Wetland became severely hydrologically fragmented by *Phragmites australis* reed beds.
2. Increasing salinity within the wetland as a result of the incremental floodgate opening trial resulted in the gradual eradication of these beds.
3. The progress of this eradication did not appear to be related to the different stages of the floodgate opening program.
4. By Stage 4 of the floodgate program, the wetland had recovered sufficiently from this infestation to have three distinct zones: a tidally fast-flowing creek section, a shallow slow-flowing spacious area including the continually overtopped creek banks, and a totally isolated freshwater, non-tidal, upper section that is partitioned from the other section by the last remaining large *Phragmites australis* reed bed.
5. Only 10% of the tidal prism of ocean water entering the Macleay River at its mouth reaches the region exterior to the floodgate and is available for tidal re-inundation.
6. A strong tidal range still reaches this external region with 75% of the ocean tidal range being available, in part because of a small tidal amplification occurring in Andersons Inlet.
7. Hydrological connectivity for the different stages of floodgate openings can be quantified by equating connectivity to magnitude of floodgate opening.

8. These stages are Stage 1—0% connectivity, Stage 2—4%, Stage 3—24% and Stage 4—63%.
9. Stage 1 exhibited a small irregular tidal cycle with a mean tidal level 0.3 m below AHD.
10. Stage 2 exhibited a larger irregular tidal cycle with a mean tidal level of the wetland's original level of approximately 0 AHD.
11. By Stage 3, the wetland had a conventional sinusoidal tidal cycle with a tidal range of approximately 0.42 m at a mean level of 0 AHD.
12. Stage 4 exhibited full estuarine characteristics with a tidal range of approximately 0.65 m compared with a tidal cycle external to the floodgates of 0.75 m.
13. Tidal ranges further within the wetland took until Stage 4 to establish a conventional sinusoidal pattern because of the losses of internal connectivity caused by *Phragmites australis.*
14. There is a quadratic relationship between tidal ranges for varying connectivities, showing that as the connectivity increased, the increases to tidal range diminished ($y = – 0.001x^2 + 0.0163x + O.1162$).
15. A comparison of connectivity and tidal flow within the wetland also shows a similar quadratic relationship with the effects of increasing connectivity having decreasing effects on the maximum tidal flow within the wetland ($y = –0.0036x^2 + 0.4166x + 0.1363$).
16. During Stage 1, there was a sharp decrease in salinity levels further upstream within the wetland, exhibiting a stepped pattern that was associated with the two blockages X and Y.
17. The salinity had reached an approximately constant value throughout the wetland by Stage 4.
18. There is a very high correlation between rainfall figures from the BOM recording station at Eungai, within the wetland catchment, and the water level heights within the freshwater section.

19. This water level height within the freshwater section indicates the state of freshwater runoff and thus is a good indicator of the chemical hydrology of the wetland.
20. The salinity within the wetland is a constant cycle of rapid decreases because of flooding followed by recovery to its original levels.
21. Salinity recovery within the wetland after flooding events is closely associated with the freshwater section water level.
22. No adverse effects of acid sulfate soils was detected at any time during the four stages including an absence of low pH levels, high toxic ion levels of aluminium, iron and sulphide, low dissolved oxygen content or 'fish kills'.

By Stage 4, December 2012, the wetland appeared to have returned to an estuarine creek status with an apparently rehabilitated biology, hydrology, and chemistry. Moreover, there are many indications of mangrove regeneration and there is clear evidence that the *Casuarina* species that replaced them are dying under the new saline conditions.

The results show that the rate of influence on the tidal range of increasing connectivity diminished as the size of the openings in the floodgate increased. This is probably the result of the increasing water flows causing a rise in the internal water levels, at any stage of the tidal cycle, resulting in lower hydraulic head height differentials across the floodgate system, which manifests as lower driving forces.

This may indicate that a small tidal re-inundation opening in the order of 25% connectivity could be sufficient to restore the original mean tidal level of approximately 0 AHD with a conventional, albeit diminished tidal cycle. It was at this stage that the wetland showed a marked change in characteristics. This increase in levels was sufficient for the tide to overtop the creek banks and cover the acid sulfate affected areas at some high tides. This appeared to be sufficient to allow for gradual, harmless removal of acid sulfate chemicals with each tide rather than allow for a build-up to occur and be released in one event during a flood.

These effects of a 24% connectivity opening were not sufficient to allow for saline water penetration of the farmland in the upper reaches of system. This system has a fortuitous barrier of *Phragmites australis* at a position in the vicinity of the extent of original mangrove vegetation, which adds further protection from saline penetration upstream.

Deleterious effects of flood mitigation programs in eastern Australian coastal wetlands, including acid sulfate soil effects, have led to the proliferation of rehabilitation programs, most of which are based on some form of tidal re-inundation. Many of these programs are a compromise between allowing sufficient tidal flow to counteract acid sulfate effects and restoring a saline environment within the wetland, and avoiding saline penetration onto agricultural land at higher tides. Most of the solutions have been in the form of some restriction to part of the tidal cycle using laterally based solutions such as drop boards and some modified form of floodgate, both of which exclude portions of the higher tidal levels (Glamore & Indraratna 2004; Indraratna et al. 2002; Johnston et al. 2005; Nelson 2006; Pease et al. 1997; Powell & Martens 2005; Streever 1998; White 2009).

Further research is recommended to evaluate the effectiveness of a tidal rehabilitation program of a coastal wetland based on the restoration with a small longitudinal connectivity opening, in the order of 25%, allowing a diminished but complete tidal cycle, which could restore enough tidal level rise to remedy the acid sulfate problem without causing upstream salinity penetration. In the absence of the protection from large *Phragmites australis* blockage, a system of small in-stream one-way floodgates would ensure the separation of the freshwater/saline water portions of the system and protect agricultural land.

CHAPTER 5

A Hydrological Predictive Model of the Salinity of the Water Entering an Enclosed Wetland during Restoration of Connectivity

5.1 Introduction

Connectivity is an important theme in ecohydrology. In particular, hydrological connectivity has been demonstrated to control the flux of energy, matter and biota into and within freshwater riverscapes and coastal estuarine wetland ecosystems (Amoros & Bornette 2002; Pringle 2003; Tetzlaff et al. 2007).

Hydrological connectivity can be used not only to construct conceptual frameworks of aquatic ecosystems structure and function but also to quantify the physical dimensions and fluxes of various ecosystem components, to enhance our understanding of ecosystem processes (Calabrese & Fagan 2004; Henein & Merriam 1990; Tischendorf & Fahrig 2000). As well as physical quantification, it is sometimes necessary to recognise the chemical quantification of hydrological connectivity, such as in the exchange of biogenic silica between tidal marshes (Struyf et al. 2006) or the inflow of agricultural lime into an acidified wetland (Johnson et al. 2009).

The need to quantify the salinity of hydrological connectivity is much more common because much of the chemistry, biology and ecology of estuarine systems is salinity dependent. Many species of estuarine flora are salinity dependent, such as mangroves (Ball & Pidsley 1995) and seagrasses (Zieman et al. 1999). *Phragmites australis* is an estuarine reed that tends to overgrow waterways at low salinity but is controlled at higher salinities (Lissner & Schierup 1999). The calcium–bicarbonate–carbonate equilibrium in seawater that is responsible for the growth of aquafauna shells is salinity dependent (Almada-Villela 1984). Toxicity of heavy metal ions to aquafauna in estuarine waters is increased at low salinities (Riba et al. 2002; Sholkovitz 1975). Many estuaries contain aquafauna that prefer specific ranges of salinity levels, such as

molluscs (Wells 1961), fish (Griffiths 2001), crustaceans (Steele & Steele 1991) and zooplankton (Lance 1964).

Many Australian rivers on the eastern coastline experience frequent flooding occurrences, which can vary in severity. When a major flooding event occurs, the magnitude of the flooding discharge exceeds that of the tidal flow, so the salinity content is flushed from the estuary region. However, much more frequent lesser flooding events occur after periods of heavy rainfall when the salinity content of the estuary is significantly lowered but may not be reduced to 0. Such estuaries experience a continuing cycle of flooding and post-flooding salinity recovery, which can vary in length from a few days to many months (KSC 2005; McInnes et al. 2002; Yeo 2002).

The estuary section of the Macleay River on the mid-north coast of NSW experiences this frequent flooding event–salinity recovery cycle. This is a study of one the tributaries of the Macleay River (Andersons Inlet) which adjoins a previously enclosed wetland system (Yarrahapinni Wetland) undergoing tidal restoration. The salinity of the water in this tributary providing the tidal input for the wetland is critical for this wetland's restoration to an estuarine environment.

The aim of this chapter is to quantify the mechanism of post-flood salinity recovery in Andersons Inlet and use this to develop a predictive model of the salinity of the water involved in the tidal restoration of the Yarrahapinni Wetland.

5.2 Study Area

The Macleay estuary is a mature barrier-dominated system in a high-energy ocean wave setting (Fig. 5.1). It is a filled delta system dominated by fluvial processes and can be broken down into three broad process zones that reflect differing degrees of fluvial and tidal interactions (KSC 2005). These are:

- fluvial process zone,
- fluvial marine transitional zone,
- marine flood tide process zone.

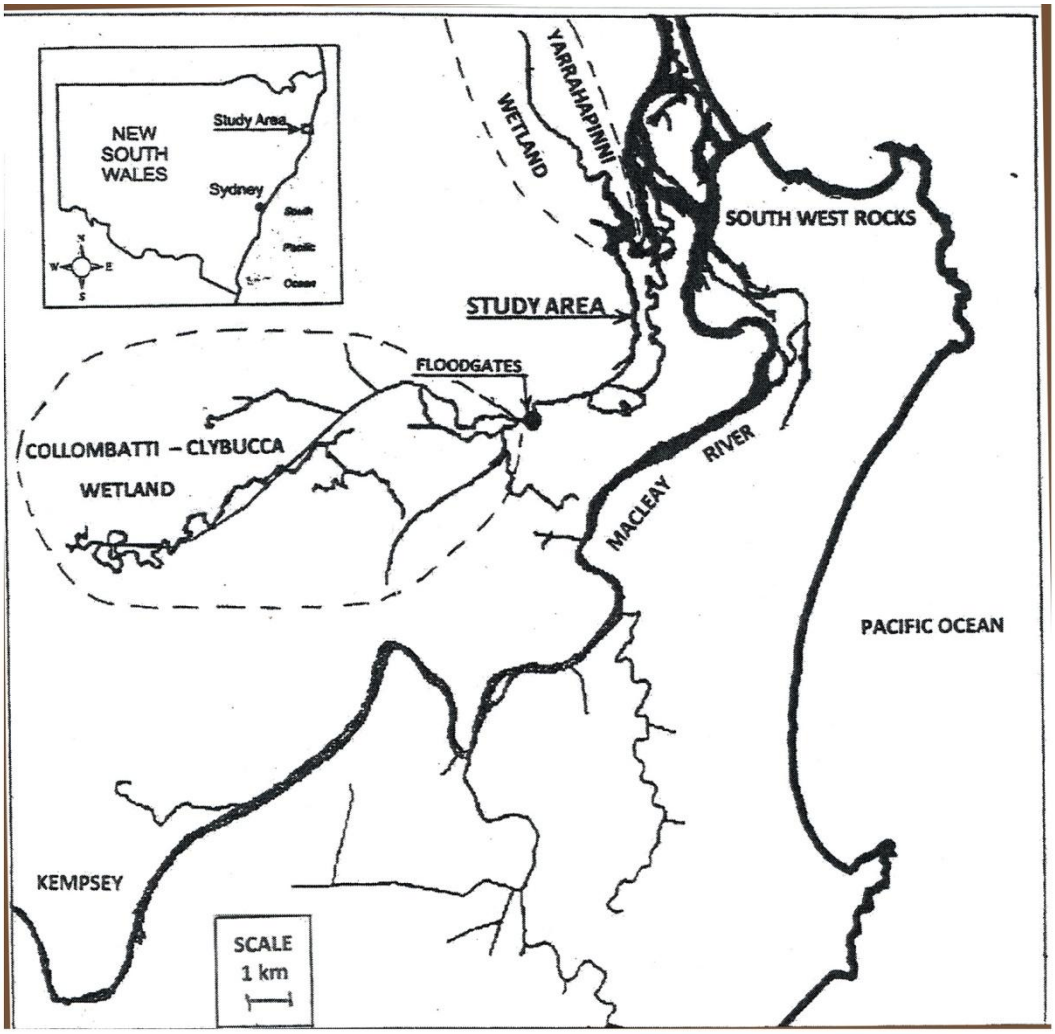

Figure 5.1: Study domain (NSW Department of Natural Resources 2009)

For this tributary of the Macleay estuary, Andersons Inlet, the fluvial zone extends from the tidal limit (near Kempsey), through the Collombatti–Clybucca wetland to the region of the 'new channels' in Andersons Inlet (Fig. 5.2). The transitional zone is small in this tributary, and most of the tributary below this new channel region falls within the marine tidal delta zone. Andersons Inlet is approximately 10 km long, with an average width of 150 m and an average depth of 2 m. The banks of the lower section and most of the new channel sections are lined with mangroves, changing to casuarina and thinning to open farm pasture near the Clybucca floodgates. The estuary supports a small crab trapping and fishing industry, the lower half is an important part of the local oyster industry and the whole region is popular for recreational fishing.

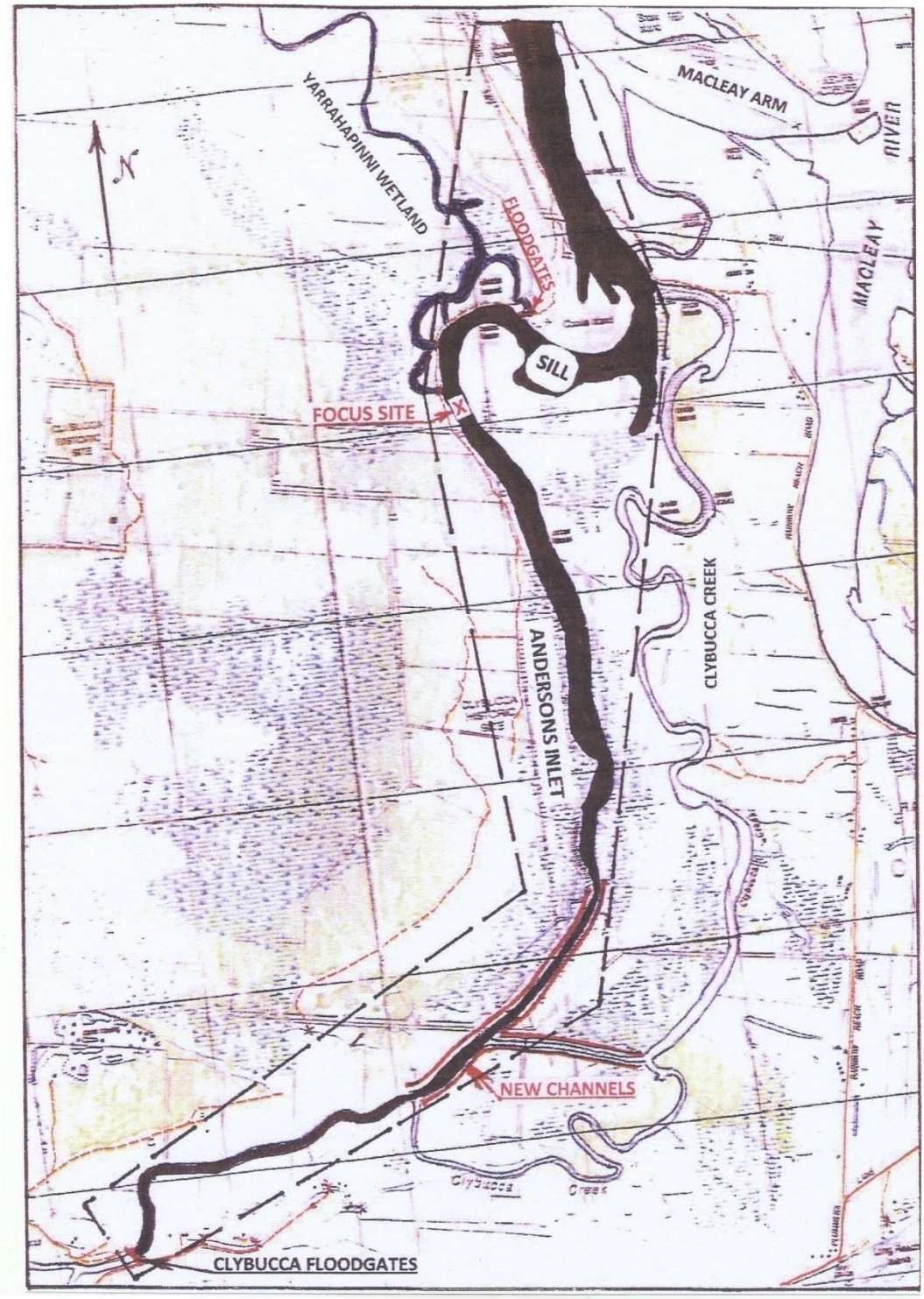

Figure 5.2: Andersons Inlet (LPI 2002) (scale 1 km gridlines)

Prior to 1966, Andersons Inlet (Fig. 5.2) was a 4-km long tributary of Clybucca Creek, an approximately 16-km long estuary that discharged the catchment from the

Collombatti–Clybucca wetland into the region of the Macleay River known as the Macleay Arm (Tulau & Naylor 1999). Until 1893, the Macleay Arm was the entrance for the Macleay River but is now only connected to it by an approximately 120-m wide channel, approximately 2 km from the new Macleay River entrance (Fig. 5.1 & 5.2).

Between 1966 and 1970, Andersons Inlet was modified by a series of flood mitigation works. These included the construction of a floodgate culvert at Clybucca Creek and approximately 3 km of channel that extended it to rejoin Clybucca Creek at two new locations, providing a wider and more direct path for flood discharge from the above wetland; it has now become the main estuary (Tefler 2005). This paper uses the naming system adopted by the NSW Department of Information Technology and Management (LPI 2002), whereby Andersons Inlet is now the 10-km section extending from the Clybucca floodgates to the Macleay Arm and Clybucca Creek is the bifurcated sections to the east (Fig. 5.2).

The Yarrahapinni Wetland (also known as the Yarrahinni Broadwater) was an approximately 600-ha mangrove and salt marsh wetland that was connected to Andersons Inlet via four channels, which were approximately 3.5 km upstream from the Macleay Arm (Department of Lands 1967). In 1971, as part of the flood mitigation works mentioned above, these channels were blocked off with rock wall levees and a structure with five one-way floodgates that changed the wetland into a freshwater environment. This wetland has undergone incremental floodgate removal to re-establish tidal hydrological connectivity.

The predictions of tidal inundation of the wetland as a result of these changes have focused on the depth and extent of rehabilitative inflows with no reference to their salinity (Chowdhury 2002). Since the major changes made to Andersons Inlet in the 1960s, this section of the river is now directly subject to water from the prolonged drainage, after significant rainfall events, from the Collombatti–Clybucca wetland. It is also reasonable to assume that, should major openings of the enclosing structures

occur, the quality of the water entering the system could be quite different from that before these structures were installed.

5.2.1 Tides

Results of tidal prism measurements during 2003, for various parts of the Macleay River estuary, are given in MHL Report 1250 (MHL 2004). The combined Clybucca Creek–Andersons Inlet system recorded tidal prisms of 2.01 x 10^6 m^3 (ebb) and 2.31 x 10^6 m^3 (flood), which is approximately 13% of the Macleay River total, with approximately 70% of this flow occurring in Andersons Inlet section (1.28 x 10^6 m^3 & 1.73 x 10^6 m^3). The mean tidal range for 1996–1999 at Cockle Island (350 m downstream from the Yarrahapinni floodgates) was 0.79 m compared with 0.84 m inside the Macleay River entrance, and the mean tidal phase lags were 82 minutes (Cockle Island) and 38 minutes (South West Rocks), compared with ocean values (MHL 2001).

5.2.2 Rainfall

Almost all of the freshwater input into the estuary comes from rainfall in the adjacent catchments of the two wetlands mentioned above. The Collombatti–Clybucca wetland has a catchment of 99.5 km^2 to the southwest of the estuary and drains via Collombatti Creek and the Seven Oaks Drain to the 21-floodgate structure at Clybucca. During severe flooding, floodwater from the main Macleay River flows overland and discharges through Andersons Inlet. The Yarrahapinni Wetland has a catchment of 60 km^2 to the northwest of the estuary and drains via Borirgalla Creek to the five-floodgate structure, 3.5 km from the estuary entrance (Fig. 5.2). This wetland plays a lesser role in influencing the salinity of Andersons Inlet because of its smaller catchment, proximity to the entrance and isolation from the main Macleay River estuary.

The 128-year mean rainfall for Kempsey (BOM Station 59017), which is adjacent to the catchment area of the Collombatti–Clybucca wetland, is 1215 mm with a monthly

mean high of 156 mm for February and a low of 56.2 mm for September. The five weather systems recognised as being responsible for flooding on the Macleay River and when they are most likely to occur are (KSC 1999):

- east coast low pressure systems (cooler months),
- rain depressions (ex-Queensland cyclones),
- monsoonal low pressure systems (late summer and autumn),
- sequences of fronts (all year round),
- high-intensity convective thunderstorms (summer).

These systems have differing seasonal and frequency probabilities, which obscures any flood prediction pattern.

For this study, the term 'rainfall event' refers to the total rainfall recorded at Kempsey (BOM Station 59017) over a three-day period. Records of the electrical conductivity at the Clybucca floodgates (KSC 2009), data logger readings and water profiling data indicate that a minor rainfall event of 40 mm can be sufficient to cause significant decrease in salinity levels in Andersons Inlet. Major rainfall events in excess of 100 mm are usually sufficient to flush the salinity content from the entire Andersons Inlet estuary. The decrease in salinity resulting from a particular rainfall event varies significantly with that event's proximity to another. A comparison of rainfall and the flooding severity for 2009, as shown by water level within the Clybucca wetland, is presented in Appendix B. During the 10-year period 2000–2009, there were 20 major rainfall events and 59 minor rainfall events, and these were more common in the first six months of the year. These events do not necessarily coincide with flooding events in the main Macleay River estuary, and Andersons Inlet may react independently, depending on the rainfall distribution. The rainfall of 2695 mm for the study period from August 2008 to December 2009 was well above the 17-month mean of 1615 mm. During this period, there were five major rainfall events and nine minor events. However, there was a prolonged period with no significant rainfall, from July to October 2009, enabling data collection for a period of extensive salinity recovery.

5.3 Methods

Numerous studies have developed predictive models of salinity intrusion into an estuary or salinity recovery after a flooding event. Parsa et al. (2007) presented an evaluation of a comparison of a one-dimensional computer model (Mike-11) with seven empirical models for salinity intrusion length, for a similar study for saltwater intrusion in the Bahmanshir estuary (Iran). Savenije (1993, 2005, 2006) developed a one-dimensional exponential model of salinity intrusions in estuaries from observations of 45 estuaries worldwide, which has been successfully applied to estuaries of widely differing structures. Schacht (2005) developed a simple exponential model of the recovery rate of an Australian east coast estuary (Fitzroy River) after a flood event by monitoring the movement of the 31% isohaline. Gillibrand and Balls (1998) developed a model of salinity intrusion for a similar-sized estuary (Ythan River, Scotland, 11 km long), from the solution of differential equations for mass, volume and momentum.

Andersons Inlet has some unique topographical and hydrological features that render these approaches to a predictive model unsuitable. These are:

1. Freshwater inflow: All of the above-mentioned experimental approaches require the establishment of a single value for freshwater inflow at one end of the model channel. This estuary has two widely separated inputs, both of which are controlled by a one-way floodgate structure. This estuary does not have regular seasonal inflows, such as a monsoon season or glacial melting, and the rainfall in its catchment areas exhibits no simple predictable pattern.
2. Seawater inflow: These models also require a value for salinity inflow and this is usually assumed to approximate seawater. This estuary does not adjoin the ocean but is a secondary tributary that merges with the Macleay Arm, which is itself a tributary of the main Macleay River. Therefore, the salinity inflow is a consequence of the interaction between these three estuary sections, so it is variable during a flood recovery cycle and difficult to predict.

3. Cross-sectional area: Many of the models require an assumption of the variation of the cross-sectional area along the length of the model channel that the area is constant or varies constantly. This estuary has three sills (broad shallow areas) along its length that cause discontinuities in cross-sectional area quantification (see Section 5.4).

These deviations from the parameters of existing models result in the need to develop an empirical model for this estuary. The aim of this study is to analyse the salinity recovery within Andersons Inlet estuary following flooding events by isohaline analysis and to develop a predictive model of the water quality outside but adjacent to the Yarrahapinni Wetland to quantify the salinity of rehabilitative inflows.

The experimental method used in this study was to record the salinity changes, both vertically and longitudinally, for the entire Andersons Inlet estuary during a 126-day period in 2009 with no significant rainfall, which followed a major flooding event. Data from the recordings were used to produce salinity contour diagrams to quantify the pattern of salinity in this estuary and to develop a predictive model for the salinity of the water entering the Yarrahapinni Wetland. These data were obtained by the three main methods discussed below.

5.3.1 Data Loggers

Seven Odyssey Salinity and Temperature, 0 to 80 millisiemen, data loggers were deployed from August 2008 to December 2009. The loggers were either housed in 50-mm PVC pipe with drilled holes attached to posts or attached to buoyed anchors, for both top and bottom readings. Bottom readings were made at 2.0 m below mean sea level (MSL) where possible.

Two of the loggers were positioned at the top and bottom recording positions at the focus site outside the Yarrahapinni Wetland to provide data for the salinity prediction model. Five loggers were deployed to supplement the salinity profiling survey and continuously moved throughout the full length of the estuary. These enabled critical

salinity changes to be followed and information to be gathered to enable selection of the optimum dates for profile sampling.

Calibration of the data loggers was maintained in situ using a Hydrolab Quanta hand-held water monitor.

5.3.2 Salinity Profiles

Salinity profiles were performed primarily using the 'moving boat method' (Savenije 2005) of following the high-water slack tidal wave (plus or minus 30 minutes), using an outboard-powered dinghy. Salinity was recorded using a YSI EC300 hand-held salinity and temperature meter at 0.5-m depth intervals, at numerous sampling sites over the entire length of the estuary. These profiling site locations were also varied for maximum data coverage during the different stages of the flood–recovery cycle but were usually less than 300 m apart on any sampling run, with the upper and lower estuary sections sampled on consecutive days. Salinity profile readings have to be recorded promptly with this method to keep pace with the slowly moving peak of the high tide as it moves up the estuary, so a fast-reacting, single reading of salinity measured in ppt is preferable. These salinity units are used throughout this paper and the conductivity units from the data loggers are temperature corrected and converted using a conversion factor of 0.64.

5.3.3 Recorded Data

Data of historical or current conditions of the estuary and surrounding regions was also used with these experimental results. The main sources were:

1. KSC website for water quality and level readings (KSC 2009),
2. Australian BOM website and archives for rainfall and river heights (BOM 2009)—recording station identification number is acknowledged when quoted,
3. MHL reports as acknowledged.

5.3.4 Statistical Analysis

Non-linear regression analysis and curve fitting analysis were performed using the SigmaPlot TableCurve 2D program.

5.4 Results

The salinity recovery after the June 2009 major rainfall event (166 mm over four days), which occurred during this dry period, is represented in Figure 5.3 (a) (lower half estuary) and (b) (upper half estuary). These diagrams show longitudinal cross-sections of the estuary with salinity isohalines represented as the boundaries between the indicated colour zones at representative time stations. Day 0 was chosen as the first day after rainfall cessation, and the diagrams of subsequent days were chosen as examples of significant changes in the salinity distribution in the estuary. Depth readings are relative to MSL. The salinity profile readings were made at the peak of high tide, and data logger readings indicate that these salinity concentrations may only occur for very short periods (less than one hour) at the crest of the tide, with the degree of duration increasing as the salinity recovery proceeds.

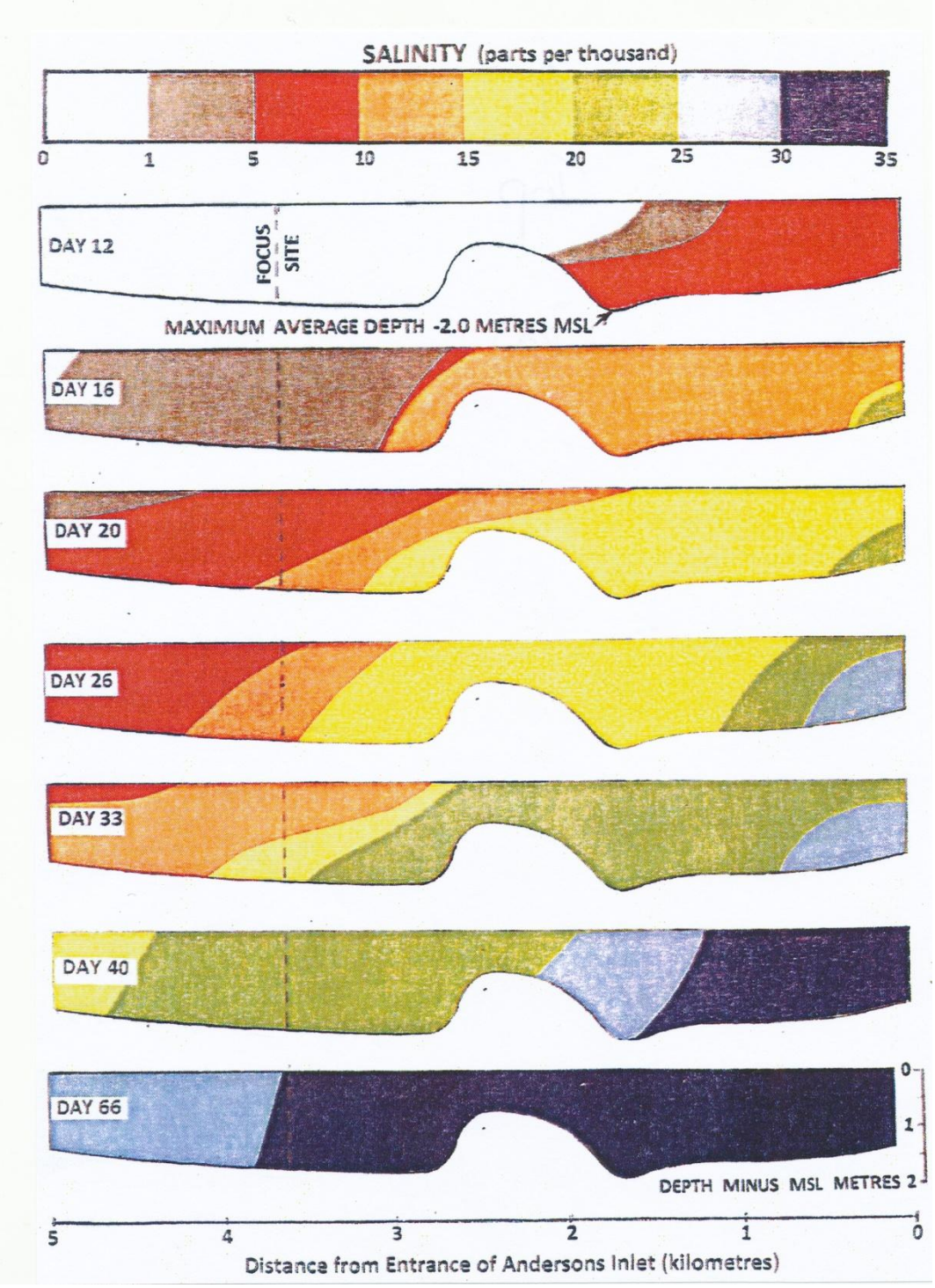
SALINITY (parts per thousand)
0
1
5
10
15
20
25
30
35
DAY 12
FOCUS SITE
MAXIMUM AVERAGE DEPTH -2.0 METRES MSL
DAY 16
DAY 20
DAY 26
DAY 33
DAY 40
DAY 66
0
1
2
DEPTH MINUS MSL METRES
5
4
3
2
1
0
Distance from Entrance of Andersons Inlet (kilometres)

(a)

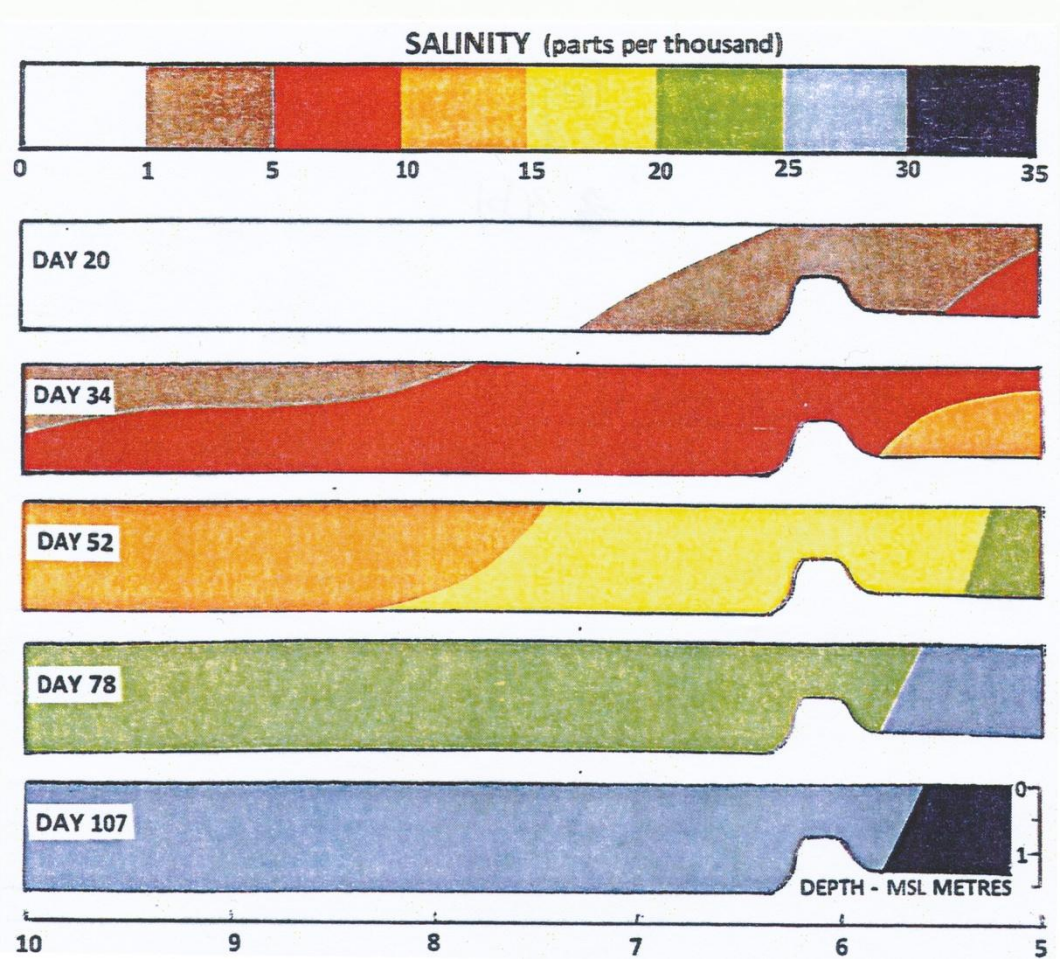

(b)

Figure 5.3: (a) Longitudinal isohaline diagrams of salinity in the lower half of Andersons Inlet, (b) isohaline diagrams of salinity in the upper half of Andersons Inlet

The slopes of the isohalines indicate that the estuary can be classified as a combination of well-mixed and partially mixed estuary with some salt wedge effects in the vicinity of the intermediate sill. The complex water flow patterns associated with submerged estuary sills have been examined both for sills associated with fjord-like inlets (Caceres et al. 2006) and for coastal plain estuaries (Blanton et al. 2000). A primary effect of such sills is turbulence resulting in estuarine mixing, which is evident in this estuary.

A major sill commences at approximately 2 km from the estuary entrance and extends for approximately 250 m. This sill consists of a sandbar extending across the entire river width, with an average depth of –0.6 m MSL, with no distinct channel but a slightly deeper area mid-width. There are increased tidal velocities across the sill because of the low depths and very evident turbulence on the down-flow margins of the sill. This sill plays a dominating role in both the discharge of floodwater and the recovery of the salinity content of the estuary because of its obstructive effects on the water flow. During the early stages of the flood–recovery cycle, the discharging floodwater has a higher velocity across the sill than the incoming higher salinity tidal flow for a major part of the tidal cycle. The velocity of the floodwater across the sill decreases during the recovery process, allowing the incoming tidal water to play an increasing role.

Savenije (1993, 2005, 2006) and Gillibrand and Balls (1998) both use salinity versus distance from estuary mouth as validation of their predictive salt intrusion models. In all cases, the diagram curves are continuous and approximate a negative-gradient straight line. Savenije (2005) proposed a method of estuarine classification based on the deviation of these continuous curves from a straight-line format. A salt intrusion curve for Andersons Inlet for 19–20 July 2009 is shown in Figure 5.4 (a) and compared with an example curve from Nguyen and Savenije (2006) for 7 April 1998 for the Mekong Delta, Vietnam. This diagram illustrates the dominating effect of the sill on salinity recovery with a distinct discontinuity at the sill region. The different slopes indicate that the two sections of the estuary recover at different rates.

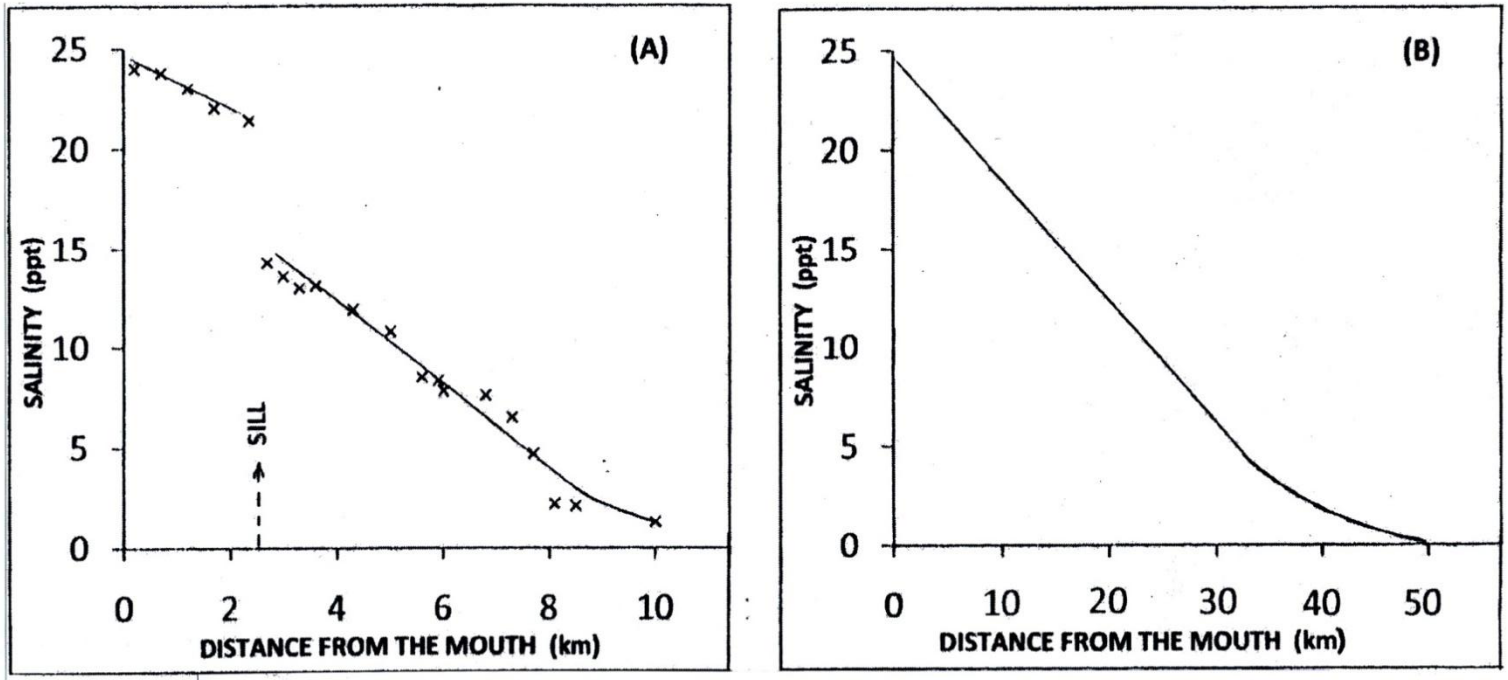

Figure 5.4: Longitudinal salinity distribution curves for (A) Andersons Inlet
(B) Hau estuary, Vietnam, from Nuygen & Savenije (2006), Fig 7c.

There is a partial sill at the entrance to the estuary in the form of a broad shallow sandbar with a navigation channel on the eastern side occupying approximately 25% of the estuary width. Another partial sill exists in the upper half of the estuary, as shown in Figure 5.3 (b). This sill was formed by blasting through a deposit of coffee rock to extend the terminating estuary during the flood mitigation modifications (KSC 2005). It also has a navigation channel on its eastern bank for approximately 25% of the estuary width. Neither of these two partial sills appear to have a significant effect on the mixing of the estuary, probably because of the presence of a significant channel area.

5.4.1 Salinity Predictive Model

A 126-day dry period commencing 21 June 2009 was monitored continuously by both bottom (–2.0 m MSL) and floating surface data loggers. The bottom salinity was generally slightly higher than the surface readings, as depicted in the isohaline diagrams, but also indicated occasional short higher salinity peaks. In addition, the Yarrahapinni Wetland is a very shallow structure, so the surface results were chosen to best represent tidal rehabilitation inflows. High-water surface readings were also subject to these short-term, higher salinity fluctuations so results for the development of a predictive model were chosen from the low-water surface readings. The readings for low water also showed significant fluctuations proportional to the range of that part of the tidal cycle. These results were filtered by only using the salinity recordings occurring for predicted results (DECC 2008, 2009) of low tide heights within the range of average low tide (0.486 m, MSL) $\pm$0.05 m.

Figure 5.5 shows these filtered results together with a curve of best fit. The function for this curve, using the TableCurve 2D best fit program, was found to be:

$$\text{SALINITY (S)} = 5.8 \ln \text{TIME (T)}$$

which has a non-linear correlation coefficient of determination of $R^2 = 0.95$ with these results. The axis T (days) is not the same as those in the isohaline diagrams but refers to T = 1 when the first evidence of salinity recovery occurs at the focus site at low tide.

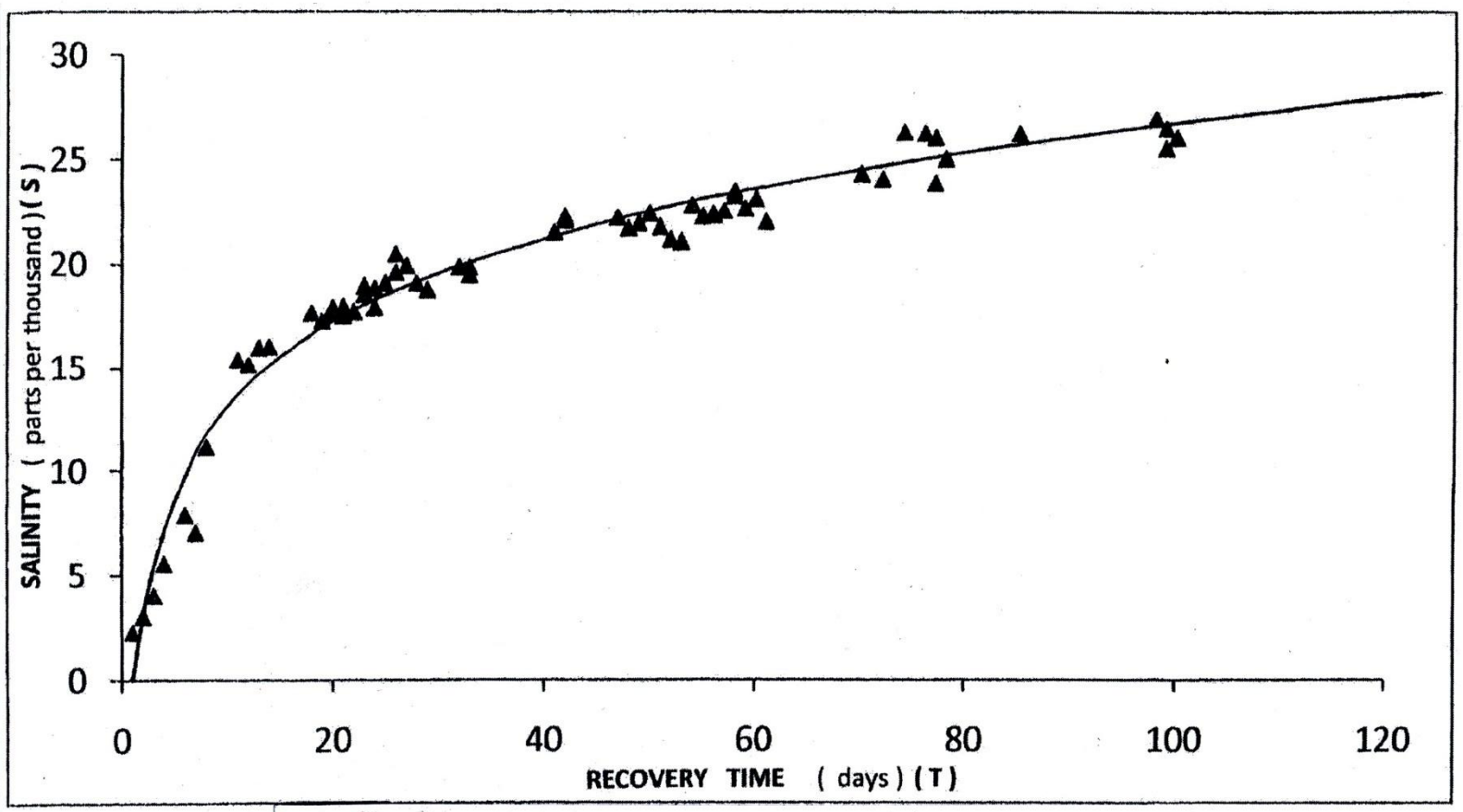

Figure 5.5: Comparison of Salinity/Recovery Time results with predicted model curve

This occurred 24 days after the rainfall ceased for this rainfall event, but this recovery time varies depending on the flooding status of the main Macleay River and the Macleay Arm, the occurrence of extreme tidal cycles and the proximity to another rainfall event. Therefore, it is not possible to incorporate the magnitude or timing of a particular rainfall event in the predictive model.

The model emphasises the prolonged nature of salinity recovery in this estuary, and the recovery times of this cycle for various definitions of recovery are shown in Table 5.1.

Table 5.1: Recovery times after recovery starts and after rainfall events for various levels of recovery salinity

SALINITY (ppt)	TIME FROM MODEL (days)	TIME AFTER RAINFALL EVENT (days)
20	31.4	55.4
25	74.4	98.4
30	175.9	199.9

It is not possible to validate this model by its application to another period of extended salinity recovery without significant rainfall because of the rarity of such an occurrence. However, there were sufficient shorter periods of recovery within the study period to enable the results from other rainfall events to be compared with the model. These results are shown in Figure 5.6, which should be viewed in conjunction with Table 5.2, which details the relevant dates for each series of recovery results. The results are filtered for average low tides and the first filtered result positioned on the model curve to provide registration for the remaining results. This overcomes the uncertainty of when recovery commences at the focus site and allows the model to be applied to both major and minor rainfall events, where recovery is only delayed. These results have a non-linear regression coefficient of determination of $R^2 = 0.81$ with the prediction model curve, which validates the proposed model.

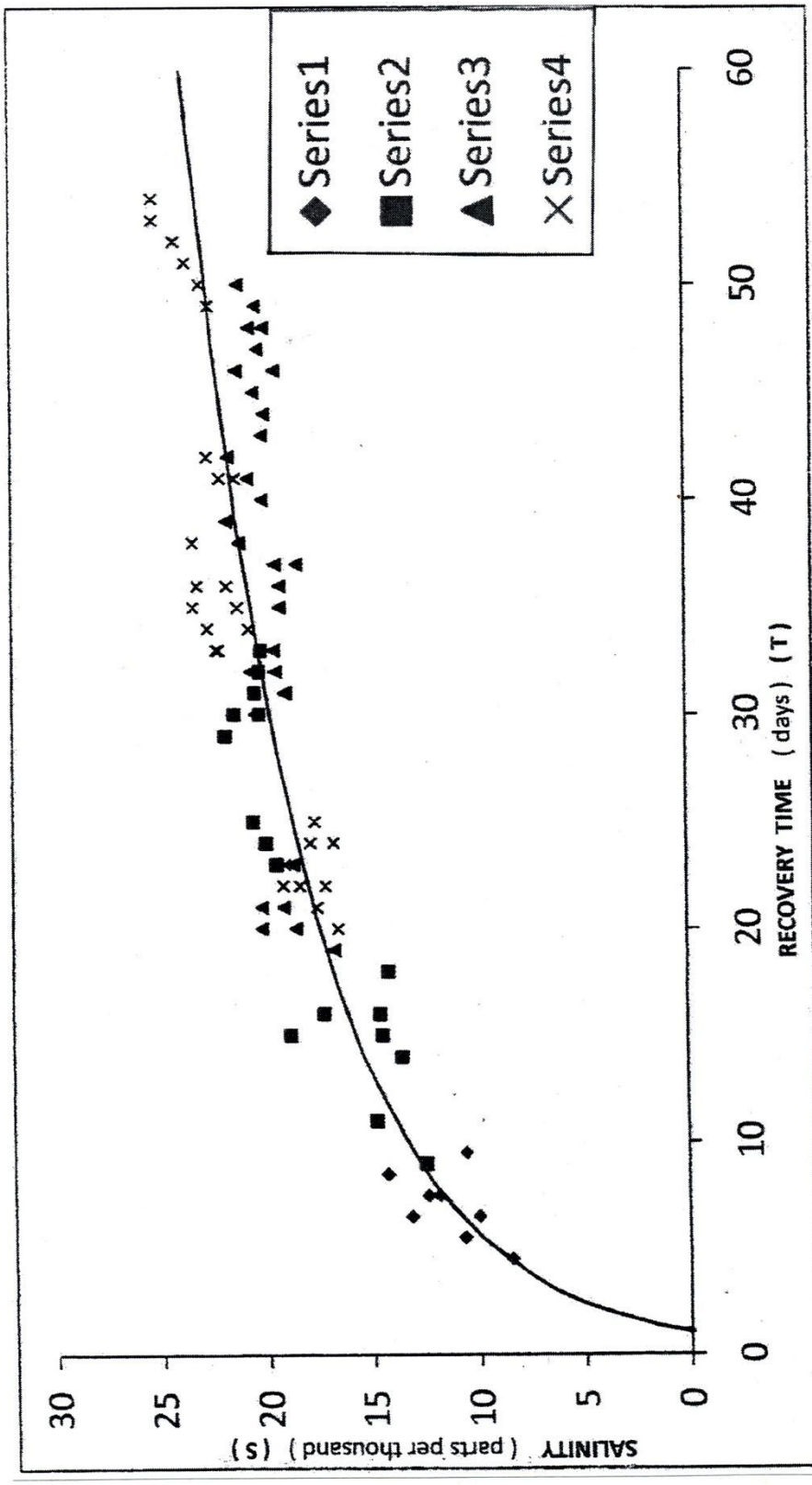

Figure 5.6: Predicted model curve compared with results from other flooding events

Table 5.2: Dates of recovery periods and first point in Figure 5.6

SERIES	START RECOVERY	FINISH RECOVERY	FIRST FILTERED DATE
1	29/4/2009	19/5/2009	9/5/2009
2	15/11/2009	14/12/2009	22/11/2009
3	27/7/2008	13/2/2009	5/1/2009
4	11/9/2008	24/11/2008	20/9/2008

5.5 Discussion

One method of classifying estuaries is based on the mechanism of the mixing of the outgoing freshwater runoff and the incoming saline seawater (University of Rhode Island 2011). The three classifications are:

- salt wedge,
- partially mixed,
- well mixed.

The term 'salt wedge' refers to the wedge shape of the freshwater–salinity interface (isohaline) where the more dense saline water moves inland beneath the less dense outgoing fresh water. Well-mixed estuaries exhibit almost vertical isohalines, and partially mixed estuaries exhibit the shapes in between the other two.

Isohaline Figures 5.3 (a) and (b) indicate that this estuary exhibits regions of all three classifications. There are significant salt wedge effects on both the upstream and downstream sides of the intermediate shallow sill. The isohalines for days 12 to 33 (Fig. 5.3 [a]) show that the salinity recovery is regarded as the deeper, more dense, saline water has to rise to the surface layers over the sill and compete with the fast floodwater discharge. It should be remembered that these diagrams represent readings taken at the peak of the high tide, and the salt intrusions upstream of the sill may only occur for a small portion of the flood cycle. Once the tide starts to ebb, the fresh water flushes the saltwater from the upper section, as was confirmed by the data logger readings at the focus site, for the early recovery period (Ibanez et al. 1997).

The construction of artificial sills is used as a mechanism to inhibit salt intrusion into estuaries when the water upstream from the sill is intended for human and agricultural consumption (Kasai et al. 2010).

Salinity–distance diagrams in Figure 5.4 reinforce that this estuary suffers from discontinuity of salinity recovery at the intermediate sill. These diagrams provide a clear explanation of the poor salinity recovery rate of Andersons Inlet at the focus site, outside the Yarrahapinni Wetland and upstream from the intermediate sill.

The salinity intrusion models referred to above would all be applicable to any estuary with a barrier, such as a sandbar, at its entrance, as often occurs. Application of these models to an estuary with an intermediate barrier is best achieved by regarding the estuary as two separate entities and applying the models independently to each section (Sotthewes & Savenije 2008).

The predictive model developed in this paper avoids this complication by being specific to the focus site outside the Yarrahapinni Wetland. The knowledge of the effects of the sill explains the rapid changes to salinity that sometimes occurred during a single tidal cycle (see Appendix C). It also justifies filtering the readings to an average tidal range and using the more stable low tide readings to develop the model.

5.6 Conclusion

The catchment runoff for the Andersons Inlet estuary is primarily controlled by one-way floodgate structures installed as part of flood mitigation programs. Such structures prolong the discharge of rainfall because discharge is controlled by the hydrostatic pressure differential across the floodgate. The catchments are subject to multiple rainfall events in any year, of sufficient intensity to cause a significant decrease in the salinity of the estuary or total flushing. The estuary was monitored for salinity content, for a 17-month period commencing August 2008, using data loggers and an extensive program of salinity profiling, over the entire estuary length.

A large intermediate sill, 2 km from the estuary entrance, plays a dominating role in salinity recovery, resulting in different recovery behaviours for its downstream and upstream segments.

The tidal prism magnitudes for the whole estuary system indicate that the majority of the discharge from the Collombatti–Clybucca, acid sulfate affected, larger wetland system flows into the Andersons Inlet branch rather than the Clybucca Creek branch, which was the only path prior to the flood mitigation works.

This estuary was subject to an abnormally high incidence of major rainfall events during the study period but did experience a prolonged dry period during the latter half of 2009. The estuary was continuously monitored for salinity during this period, at the focus site, which was chosen because it is adjacent to a proposed opening into the Yarrahapinni Wetland. These results sometimes exhibited large fluctuations during tidal cycles and between different tidal cycles, requiring filtering to eliminate anomalies. The resulting data were used to develop a predictive salinity model for this site, at low tide:

$$S = 5.8 \ln T$$

where S is the salinity (ppt) and T is the time (days) after salinity recovery commences at this site. This model was validated by comparing it with the filtered results from four other rainfall events that caused complete or partial salinity flushing in this estuary. Due to the variation in flooding rainfall leading to uncertainty of when recovery begins, it is not envisaged that this model could be used to predict estuarine salinity without calibration to a particular flooding event. A single salinity measurement of the estuarine water, at low tide, within the vicinity of the wetland would allow calibration to determine which day (T) is appropriate, so the salinity of the water entering the wetland could be accurately predicted for periods up to three months, or the next flooding event. This will be a valuable resource for a major section of this thesis: quantifying the hydrological connectivity, both in quality and magnitude, of the Yarrahapinni Wetland.

The frequency of rainfall events that significantly affect salinity, the prolonged logarithmic drainage times due to floodgates and the system being a secondary estuary all contribute to indicating that quality of the water entering the wetland will not approach that of ocean water for long periods. It is also possible that, on occasions, the water entering the wetland during rehabilitation will be comprised primarily by the discharge from the Collombatti–Clybucca wetland and will be of an inferior quality to the water within the wetland.

These factors indicate that complete rehabilitation of the Yarrahapinni Wetland can never be achieved until the problems with the discharge from the Collombatti–Clybucca are corrected.